Supporting Information

Axially Chiral Thiophene Scaffolds: Configurational Stability and Circularly Polarized Luminescence

Xinyang Li, Shuai Qiu, Wan Xu, Jia Tang, Zhiying Ma and Hua Wang**

Table of Contents

1. Experimental details

General Procedures and Materials

Ether and tetrahydrofuran (THF) for use on vacuum line were freshly distilled from sodium/benzophenone prior to use. The concentration of *n*-BuLi (in hexane) were determined by titration with *N*-pivaloyl-*o*-toluidine.[S1] Column chromatography was carried out on silica gel (300-400 mesh). Analytical thin-layer chromatography was performed on glass plates of silica gel GF-254 with detection by UV. Standard techniques for synthesis under inert atmosphere, using gasbag and Schlenk glassware equipped with an 8 mm PTFE vacuum stopcock, were employed. All starting materials and reagents were commercially available.

^{1}H NMR and ^{13}C NMR spectra were recorded on 400 or 500 MHz NMR instruments using $CDCl_3$ (7.26 and 77.00 ppm) as solvent. IR spectra were obtained using an FT-IR instrument. HRMS analysis was carried out on mass spectrometers equipped with MALDI and DART Positive Ion Mode. Melting point determination was taken on a Melt-Temp apparatus and was uncorrected. UV-vis spectra were obtained with a double-beam spectrophotometer at room temperature. The phosphorescence spectra as well as lifetime measurements were recorded on a spectrofluorometer (Edinburgh FLS980). CD spectra were recorded on Aviv Biomedical Inc Model 420SF. Circularly polarized luminescence (CPL) properties were measured with a CPL-300 spectrophotometer (JASCO). Cyclic voltammetry (CV) measurements were performed on a CHI600E electrochemical workstation (Shanghai Chenhua Instrument Co., China). All experiments were carried out with a three electrode system in a electrolytic tank under Ar at room temperature (25±1°C). Platinum electrode (a glassy carbon coated electrode with the size of 6 mm^2 × 8 cm), Pt wire (1 mm^2 × 7 cm) and Ag/AgCl electrode (by immersion into HCl/HNO_3 (3/1)) were used as the working electrode, counter electrode and reference electrode, respectively. Polishing material: Shanghai Yue ci α-alumina polishing powder (1 μm), Shanghai Chenhua polished flannel. Prior to measurements, the solvents were dried as described above and additionally degassed by five freeze-pump-thaw cycles. [nBu$_4$N][PF_6] was employed as the supporting electrolyte (0.1 M). All potential values were

referenced against the FcH/FcH^+ oxidation couple (FcH = ferrocene). Scan rates 100 mV s^{-1}. All cyclic voltammograms were plotted according to the polarographic convention. Further details were in the deposited CIF files. The fluorescence quantum yields (Φ_F) of **BDTT-Ar**s were characterized in dichloromethane with quinine sulfate (Φ_F = 0.55, 1 × 10^{-5} M in 0.5 M H_2SO_4) as a standard.[S2]

Synthesis of 2-methyl-5,5′-di(trimethylsilanyl)-3,3′-bis-dithieno[2,3-*b*:3′,2′-*d*]thiophene (BDTT-Me)

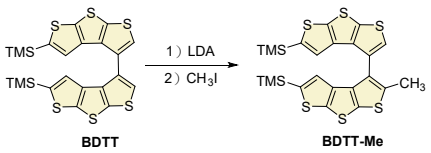

n-BuLi (2.5 M in hexane, 0.3 mL, 1.72 mmol, 2.3 equiv) was added dropwise to diisopropylamine (0.3 mL, 2.1 mmol, 2.8 equiv) in THF (5 mL) at 0 °C. After 2 h at 0 °C, the prepared LDA solution was transferred by syringe into a solution of **BDTT** (400.0 mg, 0.75 mmol) in THF (50 mL) at 0 °C. After 2 h at -78 °C, dry CH_3I (0.14 mL, 2.25 mmol, 1.1 equiv) was added at -78 °C, then warmed up slowly to ambient temperature overnight. After being quenched with CH_3OH at -78 °C, the reaction mixture was extracted with CH_2Cl_2 (3 × 20 mL), and the organic phase was washed with H_2O (3 × 30 mL) and then dried over Na_2SO_4. After the solvent was removed under vacuum, the residue was purified by column chromatography on silica gel with petrol ether as the eluent to obtain **BDTT-Me** as a white product (392.5 mg, 93%). M.p.: 181-182 °C. ^{1}H NMR (500 MHz, $CDCl_3$) δ (ppm) 7.52 (s, 1H), 6.46 (s, 1H), 6.40 (s, 1H), 2.12 (s, 3H), 0.11 (s, 9H), 0.03 (s, 9H). ^{13}C NMR (125 MHz, $CDCl_3$) δ (ppm) 144.07, 143.57, 143.42, 143.15, 140.75, 140.65, 139.59, 138.87, 138.62, 127.55, 126.96, 125.84, 125.61, 125.44, 125.30, 125.10, 13.56, -0.35. HRMS (MALDI-FT) *m/z* $[M+H]^+$ calcd for $[C_{23}H_{25}S_6Si_2]$ 548.9818; found 548.9814.IR (KBr): 3052, 1413, 1229, 976, 851, 756 cm^{-1}.

Synthesis of 2-phenyl-5,5′-di(trimethylsilanyl)-3,3′-bis-dithieno[2,3-*b*:3′,2′-*d*]thiophene (BDTT-Ph)

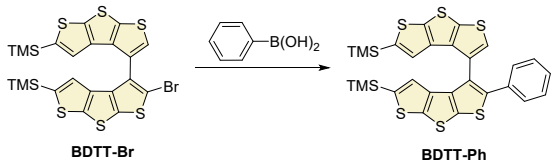

Compound **BDTT-Br** (40.0 mg, 0.065 mmol), phenylboronic acid (18.0 mg, 0.065 mmol, 1.0 equiv), $Pd(PPh_3)_4$ (1.5 mg, 0.0013 mmol, 0.02 equiv), K_2CO_3 (18.0 mg, 0.130 mmol, 2.0 equiv) and

deoxidized water (1 mL) were added into THF (10 mL). The reaction mixture was heated at 70 °C for 15 h. After cooling down to room, the reaction mixture was extracted with CH_2Cl_2 (3 × 15 mL), and the organic phase was washed with H_2O (3 × 20 mL) and then dried over Na_2SO_4. After the solvent was removed under vacuum, the residue was purified by column chromatography on silica gel with petrol ether as the eluent to obtain **BDTT-Ph** (37.7 mg, 95%) as a white solid. M.p.: 197-198 °C. ^{1}H NMR (500 MHz, $CDCl_3$) δ (ppm) 7.35 (d, J = 10.0 Hz, 2H), 7.28 (s, 1H), 7.21-7.17 (m, 3H), 6.59 (d, J = 10.0 Hz, 2H), 0.13 (s, 9H), 0.12 (s, 9H). ^{13}C NMR (125 MHz, $CDCl_3$) δ (ppm) 174.03, 143.79, 143.69, 143.52, 143.15, 142.44, 140.77, 140.20, 139.74, 138.72, 137.60, 137.00, 134.27, 128.59, 128.52, 128.32, 127.97, 127.66, 126.25, 125.88, 125.67, 123.97, -0.33, -0.35. HRMS (ESI-TOF) *m/z* $[M+H]^+$ calcd for $[C_{28}H_{27}S_6Si_2]$ 610.9970; found 610.9983. IR (KBr): 2952, 1355, 1249, 982, 835, 756 cm^{-1}.

Synthesis of 2-phenyl-5,5′-di(trimethylsilanyl)-3,3′-bis-dithieno[2,3-*b*:3′,2′-*d*]thiophene (BDTT-1Np)

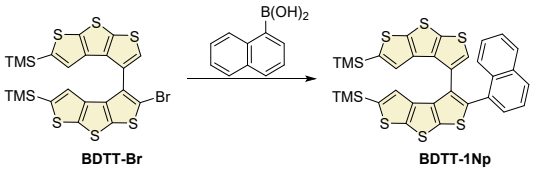

BDTT-Br BDTT-1Np

Compound **BDTT-Br** (69.0 mg, 0.112 mmol), 1-Naphthylboronic acid (21.2 mg, 0.123 mmol, 1.1 equiv), $Pd(PPh_3)_4$ (2.6 mg, 0.0023 mmol, 0.02 equiv), K_2CO_3 (30.3 mg, 0.22 mmol, 2.2 equiv) and deoxidized water (0.8 mL) were added into THF (8 mL). The reaction mixture was heated at 70 °C for 15 h. After cooling down to room, the reaction mixture was extracted with CH_2Cl_2 (3 × 15 mL), and the organic phase was washed with H_2O (3 × 20 mL) and then dried over Na_2SO_4. After the solvent was removed under vacuum, the residue was purified by column chromatography on silica gel with petrol ether as the eluent to obtain **BDTT-1Np** (61.5 mg, 83%) as a white solid. M.p.: 217-218 °C. ^{1}H NMR (500 MHz, $CDCl_3$) δ (ppm) 7.98 (d, J = 8.4 Hz, 1H), 7.83 (d, J = 5.2 Hz, 2H), 7.53 (d, J = 6.1 Hz, 1H), 7.44-7.38 (m, 2H), 7.31 (s, 1H), 6.84 (s, 1H), 6.59 (s, 1H), 6.38 (s, 1H), 0.10 (s, 9H), 0.05 (s, 9H). ^{13}C NMR (125 MHz, $CDCl_3$) δ (ppm) 143.79, 143.55, 143.12, 140.81, 140.27, 140.07, 139.25, 138.46, 137.49, 137.05, 133.44, 132.80, 132.13, 132.05, 131.95, 131.26, 129.91, 129.08, 128.55, 128.46, 128.22, 126.45, 126.29, 125.99, 125.78, 125.00, -0.34, -0.43. HRMS (ESI-TOF) *m/z* $[M+H]^+$ calcd for $[C_{32}H_{29}S_6Si_2]$ 661.0127; found 661.0120. IR (KBr): 2947,

1469, 1259, 992, 973, 756 cm^{-1}.

Synthesis of 2,2′-phenyl-5,5′-di(trimethylsilanyl)-3,3′-bis-dithieno[2,3-*b*:3′,2′-*d*]thiophene (BDTT-2Np)

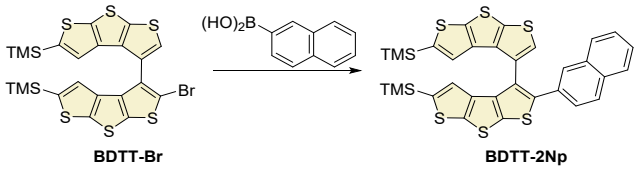

BDTT-Br BDTT-2Np

Compound **BDTT-Br** (40 mg, 0.065 mmol), 2-Naphthylboronic acid (47.3 mg, 0.072 mmol, 1.1 equiv), $Pd(PPh_3)_4$ (1.5 mg, 0.0013 mmol, 0.02 equiv), K_2CO_3 (18.0 mg, 0.130 mmol, 2.0 equiv) and deoxidized water (1 mL) were added into THF (10 mL). The reaction mixture was heated at 70 °C for 17 h. After cooling down to room, the reaction mixture was extracted with CH_2Cl_2 (3 × 15 mL), and the organic phase was washed with H_2O (3 × 20 mL) and then dried over Na_2SO_4. After the solvent was removed under vacuum, the residue was purified by column chromatography on silica gel with petrol ether as the eluent to obtain **BDTT-2Np** (34.7 mg, 80%) as a white solid. M.p.: 211-212 °C. ^1H NMR (500 MHz, $CDCl_3$) δ (ppm) 7.91 (s, 1H), 7.72 (d, J = 6.1 Hz, 2H), 7.60 (d, J = 8.9 Hz, 1H), 7.44-7.41 (m, 2H), 7.35 (dd, J = 2, 8.7 Hz, 1H), 7.28 (s, 1H), 6.63 (s, 1H), 6.59 (s, 1H), 0.13 (s, 9H), 0.08 (s, 9H). ^{13}C NMR (125 MHz, $CDCl_3$) δ (ppm) 143.89, 143.74, 143.52, 143.21, 142.47, 140.77, 140.19, 139.83, 138.75, 137.83, 137.08, 133.27, 132.53, 131.92, 128.05, 127.66, 127.64, 127.60, 127.58, 126.54, 126.51, 126.34, 126.24, 125.93, 125.79, 124.29, -0.36, -0.39. HRMS (ESI-TOF) *m/z* $[M+H]^+$ calcd for $[C_{32}H_{29}S_6Si_2]$ 661.0127; found 661.0125. IR (KBr): 2952, 1460, 1352, 1249, 984, 756 cm^{-1}.

Synthesis of 2-phenyl-5,5′-di(trimethylsilanyl)-3,3′-bis-dithieno[2,3-*b*:3′,2′-*d*]thiophene (BDTT-2An)

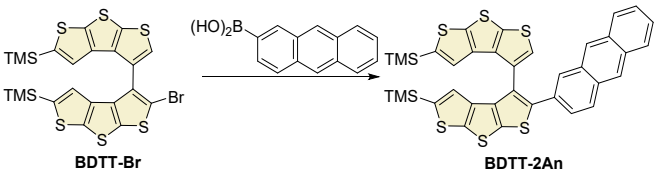

BDTT-Br BDTT-2An

Compound **BDTT-Br** (100 mg, 0.162 mmol), 2-Anthraceneboronic acid (43.4 mg, 0.195 mmol, 1.2 equiv), $Pd(PPh_3)_4$ (3.7 mg, 0.00324 mmol, 0.02 equiv), K_2CO_3 (56.0 mg, 0.405 mmol, 2.5 equiv) and deoxidized water (1.5 mL) were added into toluene (15 mL). The reaction mixture was heated at 100 °C for 24 h. After cooling down to room, the reaction mixture was extracted with

CH_2Cl_2 (3 × 15 mL), and the organic phase was washed with H_2O (3 × 20 mL) and then dried over Na_2SO_4. After the solvent was removed under vacuum, the residue was purified by column chromatography on silica gel with petrol ether as the eluent to obtain **BDTT-2An** (90.9 mg, 82%) as a white solid. M.p.: 239-240 °C. ^{1}H NMR (500 MHz, $CDCl_3$) δ (ppm) 8.30 (d, J = 6.6 Hz, 2H), 8.08 (s, 1H), 7.94 (d, J = 6.9 Hz, 2H), 7.76 (d, J = 11 Hz, 2H), 7.47-7.43 (m, 2H), 7.33-7.32 (m, 2H), 6.66 (s, 1H), 6.60 (s, 1H), 0.13 (s, 9H), 0.06 (s, 9H). ^{13}C NMR (125 MHz, $CDCl_3$) δ (ppm) 143.35, 141.10, 140.59, 139.46, 139.24, 137.85, 137.62, 137.23, 134.38, 133.84, 133.79, 131.75, 131.41, 131.17, 129.13, 129.07, 128.96, 128.64, 128.54, 127.50, 127.41, 127.13, 126.83, 126.78, 126.73, 126.59, 126.38, 126.03, 125.67, 125.51, 125.49, -0.35, -0.41. HRMS (ESI-TOF) *m/z* $[M+H]^+$ calcd for $[C_{36}H_{31}S_6Si_2]$ 711.0283; found 711.0276. IR (KBr): 2955, 1465, 1350, 1180, 977, 756 cm^{-1}.

Synthesis of 2-phenyl-5,5′-di(trimethylsilanyl)-3,3′-bis-dithieno[2,3-*b*:3′,2′-*d*]thiophene (BDTT-9An)

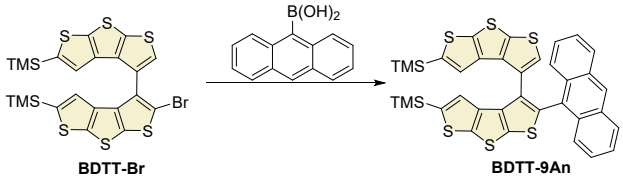

Compound **BDTT-Br** (100 mg, 0.162 mmol), 9-Anthraceneboronic acid (43.4 mg, 0.195 mmol, 1.2 equiv), $Pd(PPh_3)_4$ (3.7 mg, 0.00324 mmol, 0.02 equiv), K_2CO_3 (56.0 mg, 0.405 mmol, 2.5 equiv) and deoxidized water (1 mL) were added into toluene (10 mL). The reaction mixture was heated at 100 °C for 36 h. After cooling down to room, the reaction mixture was extracted with CH_2Cl_2 (3 × 15 mL), and the organic phase was washed with H_2O (3 × 20 mL) and then dried over Na_2SO_4. After the solvent was removed under vacuum, the residue was purified by column chromatography on silica gel with petrol ether as the eluent to obtain **BDTT-9An** (86.5 mg, 75%) as a white solid. M.p.: 262-263 °C. ^{1}H NMR (500 MHz, $CDCl_3$) δ (ppm) 8.51 (s, 1H), 8.23 (d, J = 6.7 Hz, 1H), 8.08 (d, J = 8.0 Hz, 1H), 7.92 (d, J = 8.6 Hz, 1H), 7.67 (d, J = 8.9 Hz, 1H), 7.58-7.52 (m, 1H), 7.28 (t, J = 6.6 Hz, 1H), 7.09 (t, J = 7.7 Hz, 1H), 6.67 (s, 1H), 6.61 (s, 1H), 6.27 (s, 1H), 0.12 (s, 9H), 0.03 (s, 9H). ^{13}C NMR (125 MHz, $CDCl_3$) δ (ppm) 143.61, 143.09, 140.84, 140.32, 139.20, 139.01, 137.59, 137.36, 136.97, 134.12, 133.58, 133.52, 131.49, 131.15, 130.91, 130.62, 128.87, 128.81, 128.70, 128.28, 126.87, 126.57, 126.52, 126.47, 126.33, 126.12, 125.77, 125.41,

125.25, 125.23, -0.30, -0.45. HRMS (ESI-TOF) *m/z* $[M+H]^+$ calcd for $[C_{36}H_{31}S_6Si_2]$ 711.0283; found 711.0288. IR (KBr): 2955, 1463, 1350, 1250, 939, 756 cm^{-1}.

Synthesis of 2-phenyl-5,5′-di(trimethylsilanyl)-3,3′-bis-dithieno[2,3-*b*:3′,2′-*d*]thiophene (BDTT-1Py)

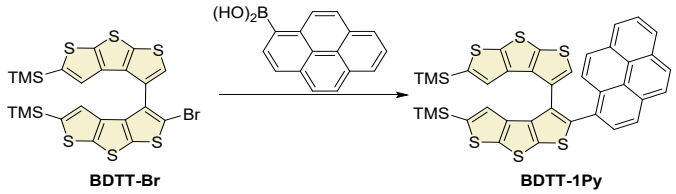

Compound **BDTT-Br** (65.3 mg, 0.11 mmol), 1-Pyrenylboronic acid (13.0 mg, 0.11 mmol, 1.0 equiv), $Pd(PPh_3)_4$ (2.5 mg, 0.002 mmol, 0.02 equiv), K_2CO_3 (36.8 mg, 0.27 mmol, 2.5 equiv) and deoxidized water (1 mL) were added into toluene (10 mL). The reaction mixture was heated at 100 °C for 20 h. After cooling down to room, the reaction mixture was extracted with CH_2Cl_2 (3 × 15 mL), and the organic phase was washed with H_2O (3 × 20 mL) and then dried over Na_2SO_4. After the solvent was removed under vacuum, the residue was purified by column chromatography on silica gel with petrol ether as the eluent to obtain **BDTT-1Py** (61.8 mg, 75%) as a white solid. M.p.: 290-291 °C. ^1H NMR (500 MHz, $CDCl_3$) δ (ppm) 8.20 (d, J = 9.5 Hz, 2H), 8.14-8.06 (m, 5H), 8.02 (t, J = 9.5 Hz, 2H), 6.82 (s, 1H), 6.67 (s, 1H), 6.40 (s, 1H), 0.12 (s, 9H), 0.06 (s, 9H). ^{13}C NMR (125 MHz, $CDCl_3$) δ (ppm) 143.79, 143.55, 143.12, 140.81, 140.27, 140.07, 139.25, 138.46, 137.49, 137.05, 133.44, 132.80, 132.13, 132.05, 131.95, 131.26, 129.91, 129.08, 128.55, 128.46, 128.22, 126.45, 126.29, 125.99, 125.89, 125.78, 125.00, -0.34, -0.43. HRMS (MALDI-FT) *m/z* $[M]^+$ calcd for $[C_{38}H_{30}S_6Si_2]$ 751.0596; found 751.0624. IR (KBr): 2952, 1403, 1350, 1249, 1113, 984, 756 cm^{-1}.

2. NMR and HRMS Spectra

NMR and HRMS Spectra of BDTT-Me

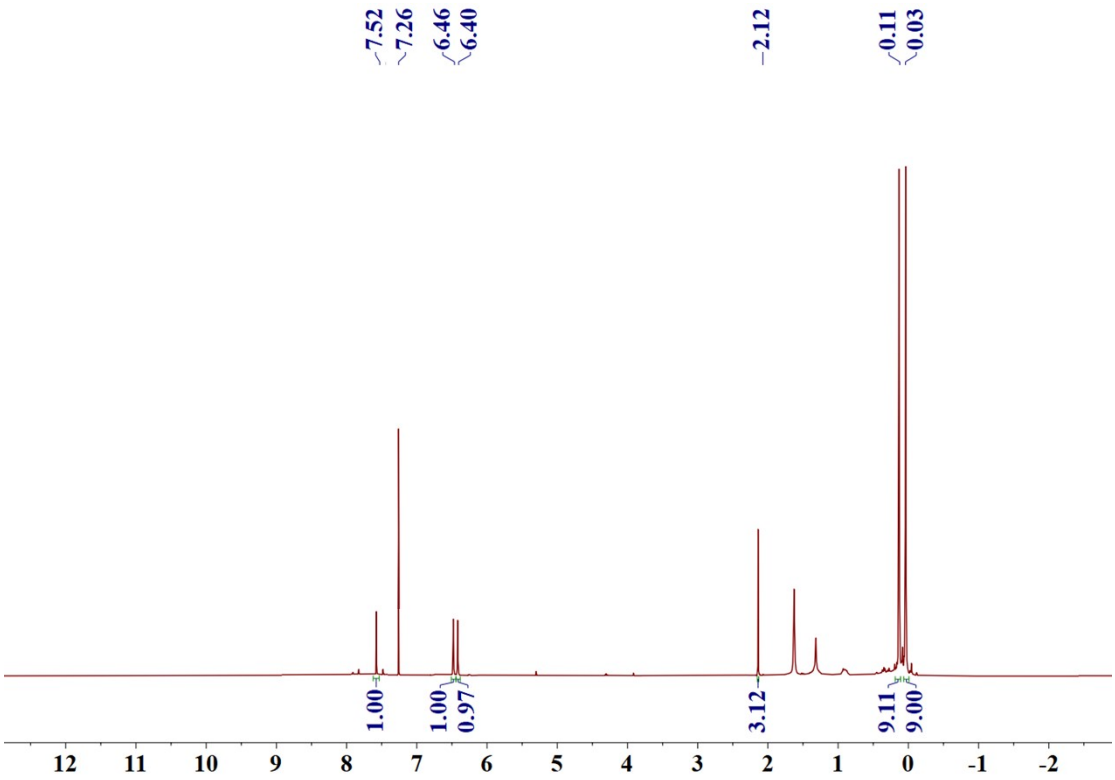

Figure S1. ^{1}H NMR (500 MHz, $CDCl_3$) spectrum of **BDTT-Me**.

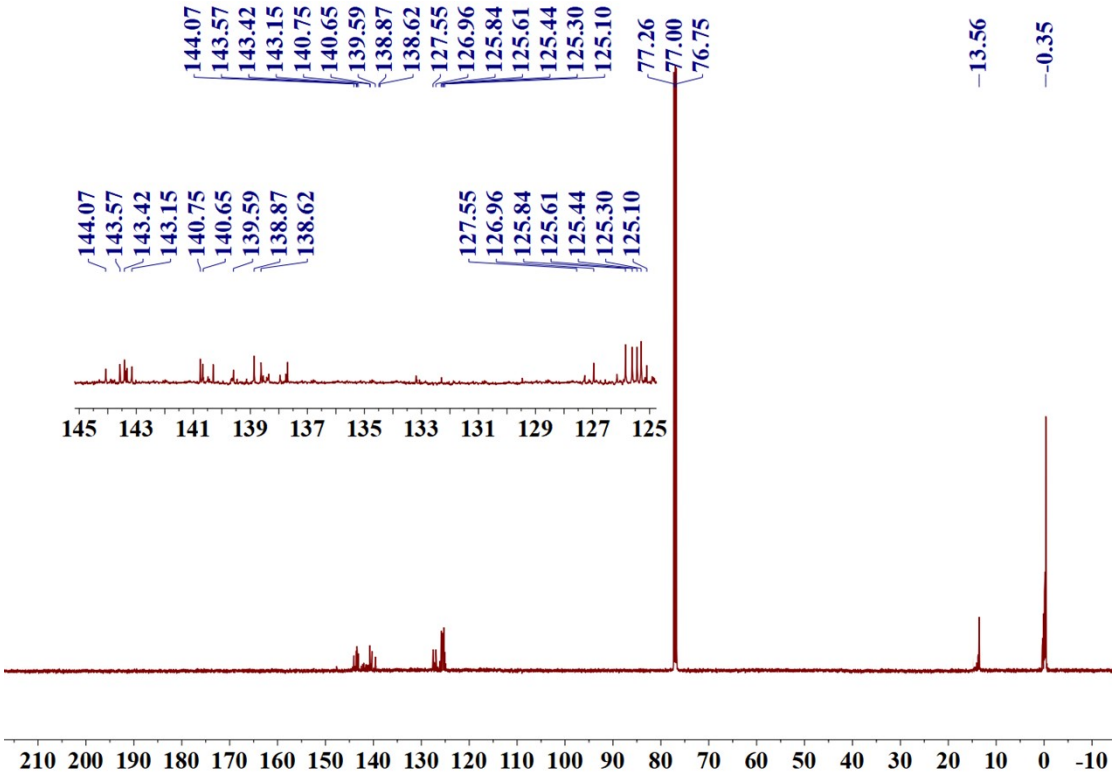

Figure S2. ^{13}C NMR (125 MHz, $CDCl_3$) spectra of **BDTT-Me**.

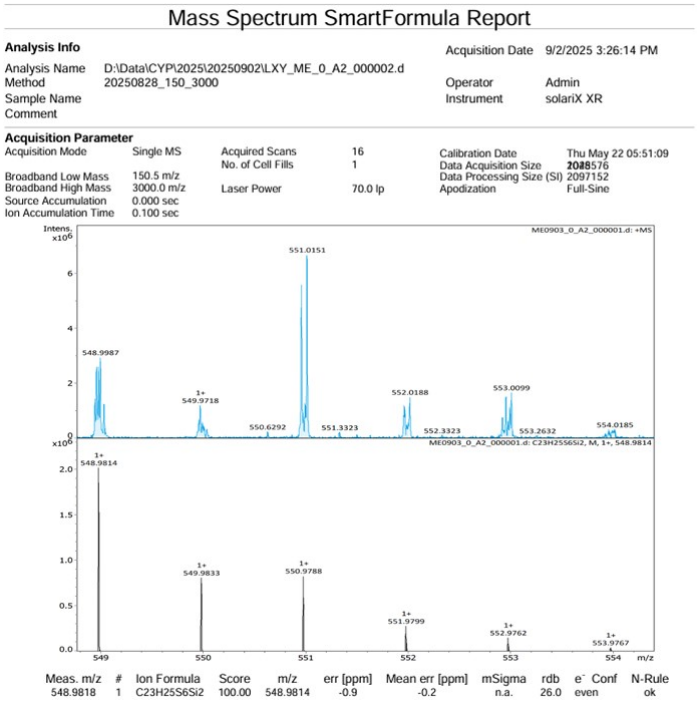

Figure S3. HRMS spectra of **BDTT-Me**.

NMR and HRMS Spectra of BDTT-Ph

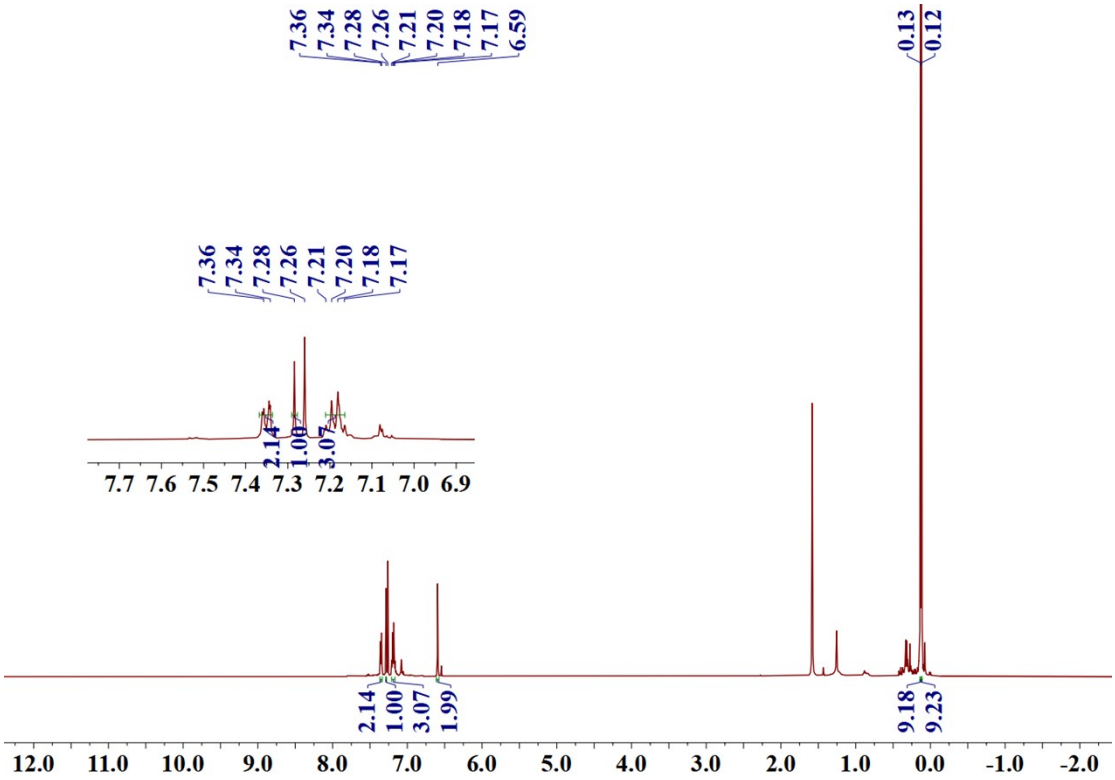

Figure S4. ^{1}H NMR (500 MHz, $CDCl_3$) spectra of **BDTT-Ph**.

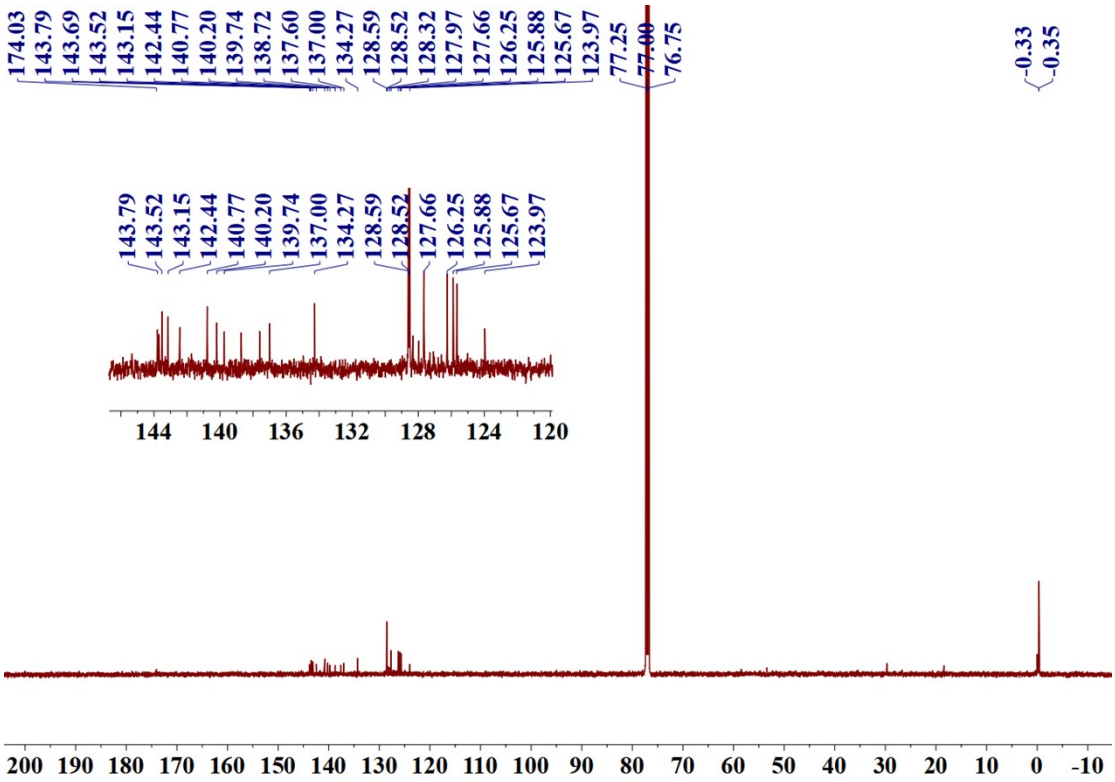

Figure S5. ^{13}C NMR (125 MHz, $CDCl_3$) spectra of **BDTT-Ph**.

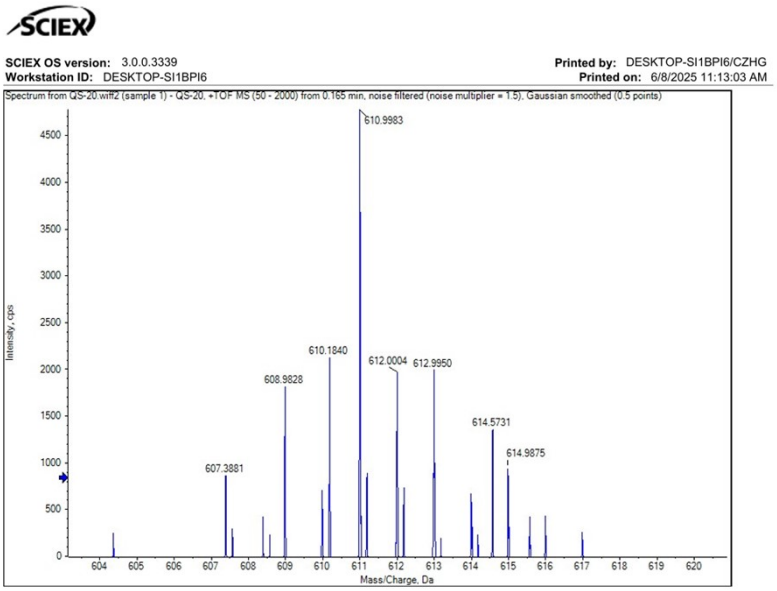

Figure S6. HRMS spectrum of **BDTT-Ph**.

NMR and HRMS Spectra of BDTT-1Np

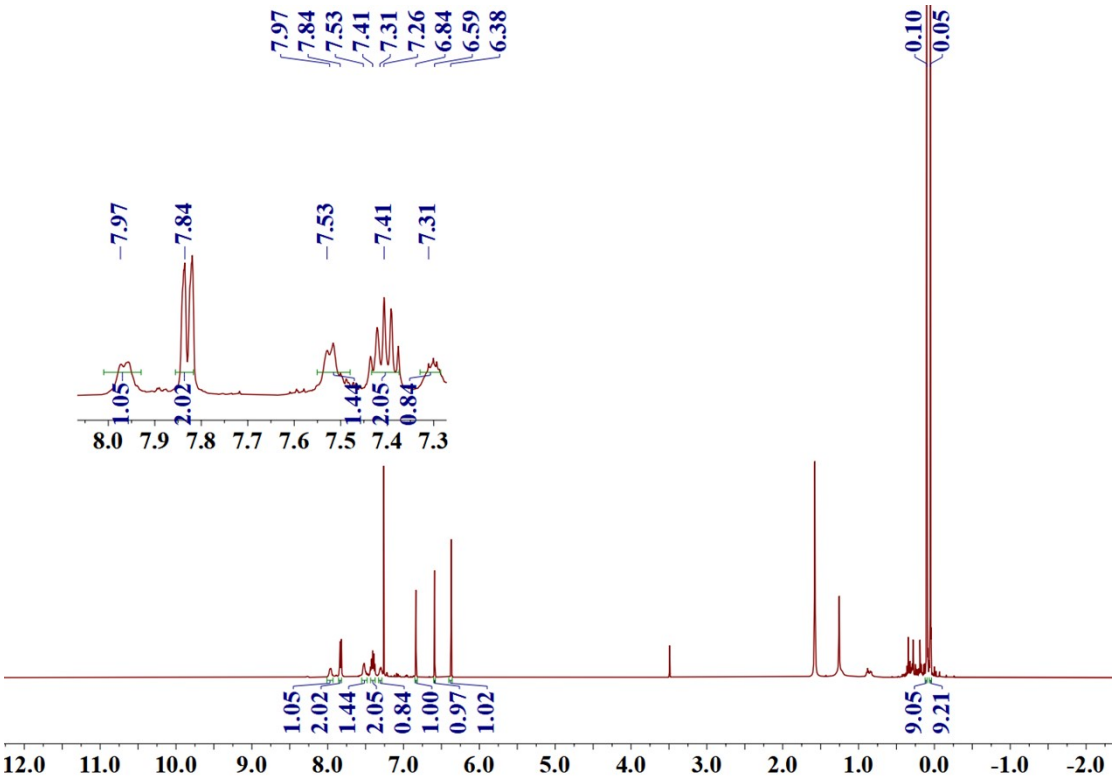

Figure S7. ^{1}H NMR (500 MHz, $CDCl_3$) spectra of **BDTT-1Np**.

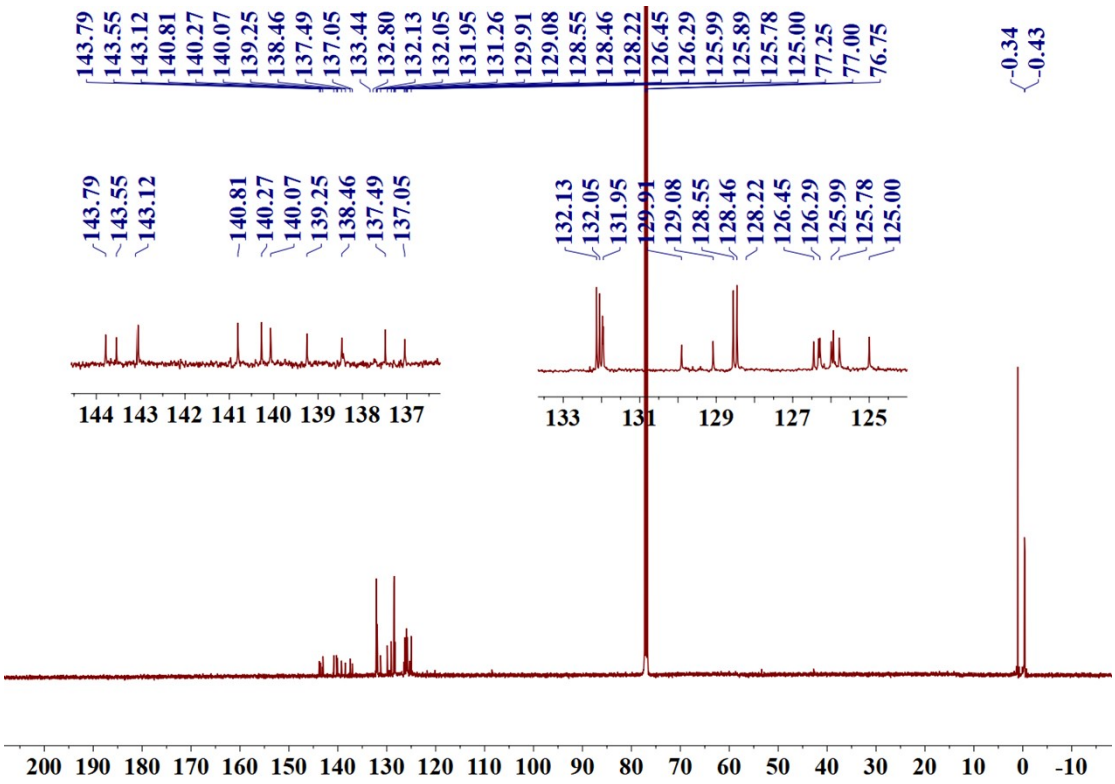

Figure S8. ^{13}C NMR (125 MHz, $CDCl_3$) spectra of **BDTT-1Np**.

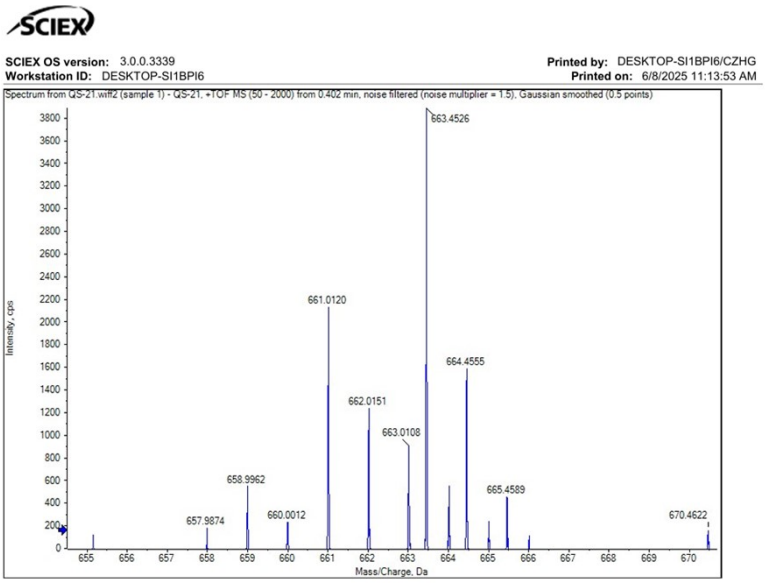

Figure S9. HRMS spectrum of **BDTT-1Np**.

NMR and HRMS Spectra of BDTT-2Np

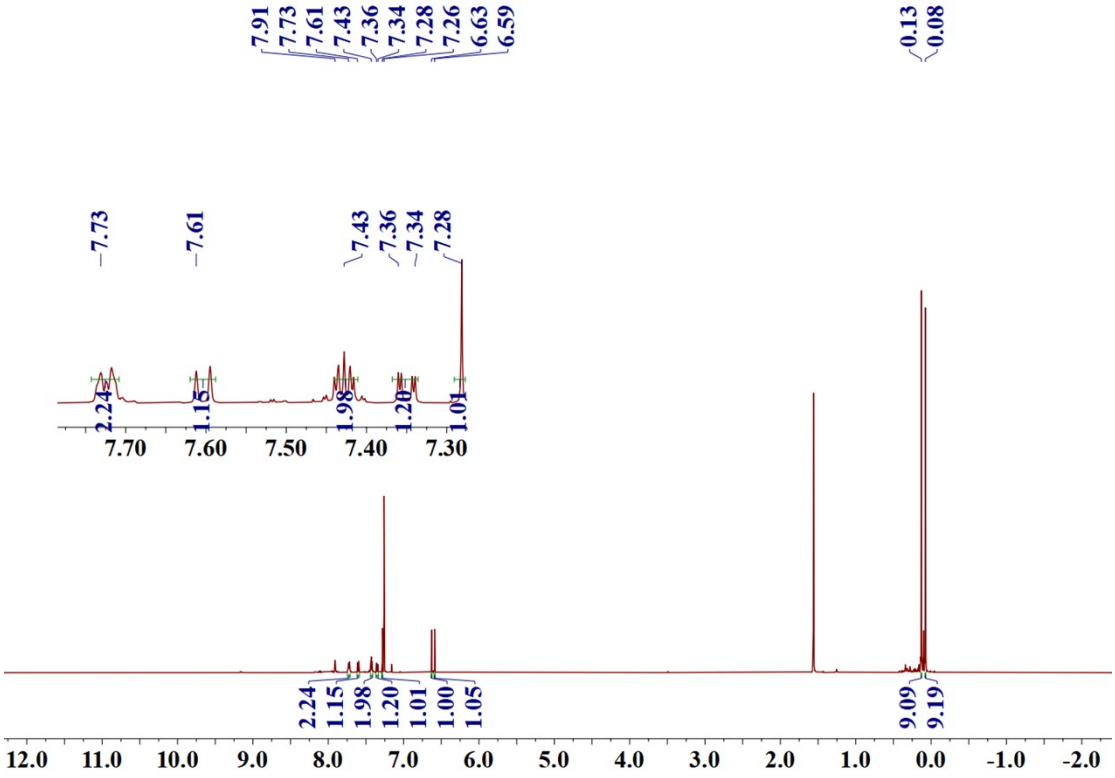

Figure S10. ^{1}H NMR (500 MHz, $CDCl_3$) spectra of **BDTT-2Np**.

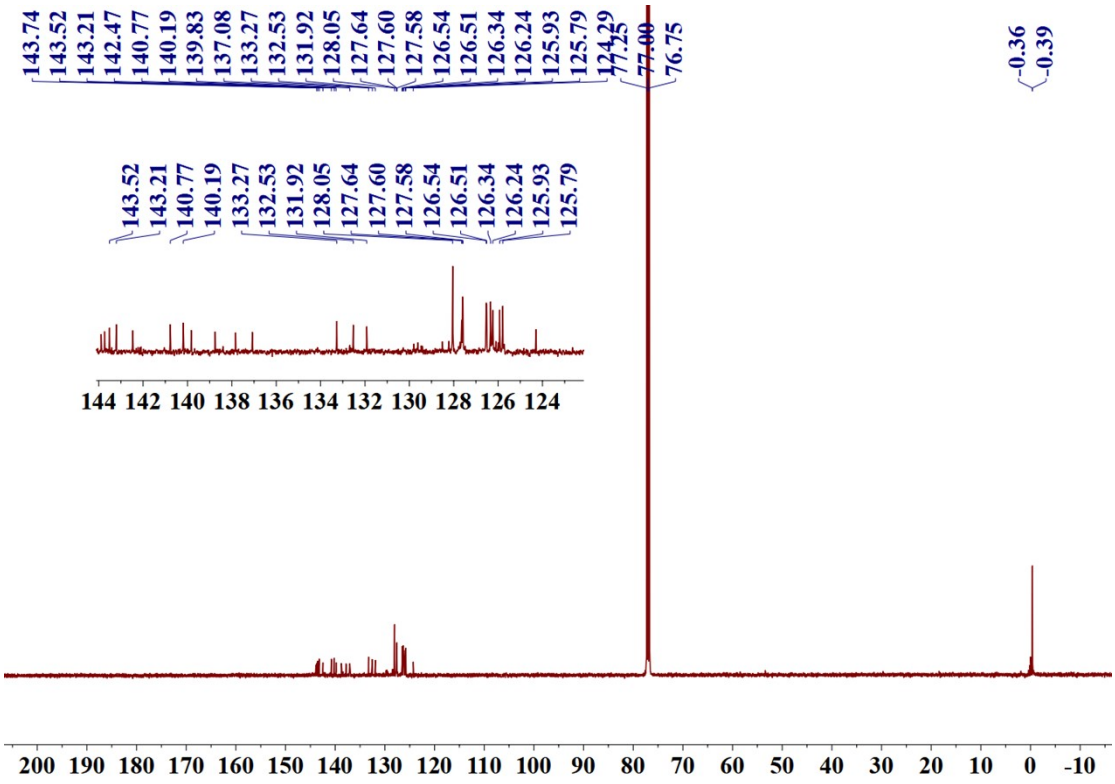

Figure S11. ^{13}C NMR (125 MHz, $CDCl_3$) spectra of **BDTT-2Np**.

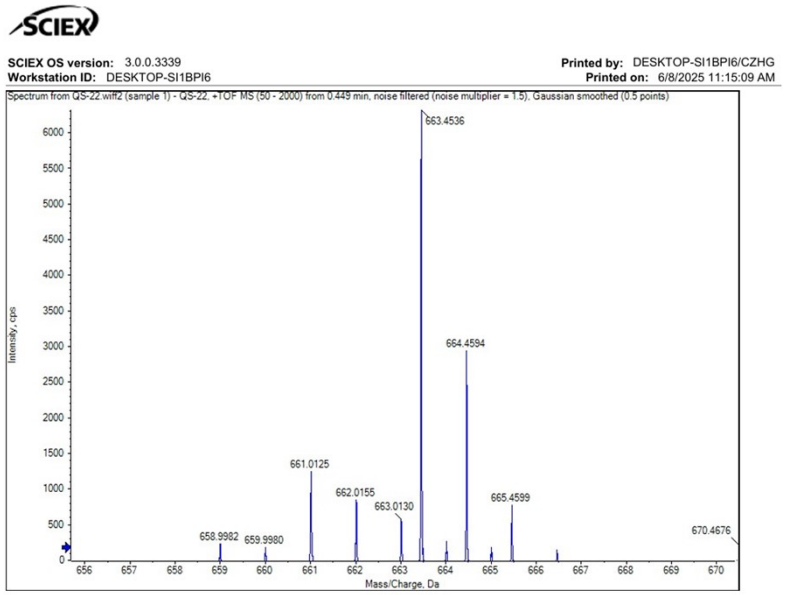

Figure S12. HRMS spectrum of **BDTT-2Np**.

NMR and HRMS Spectra of BDTT-2An

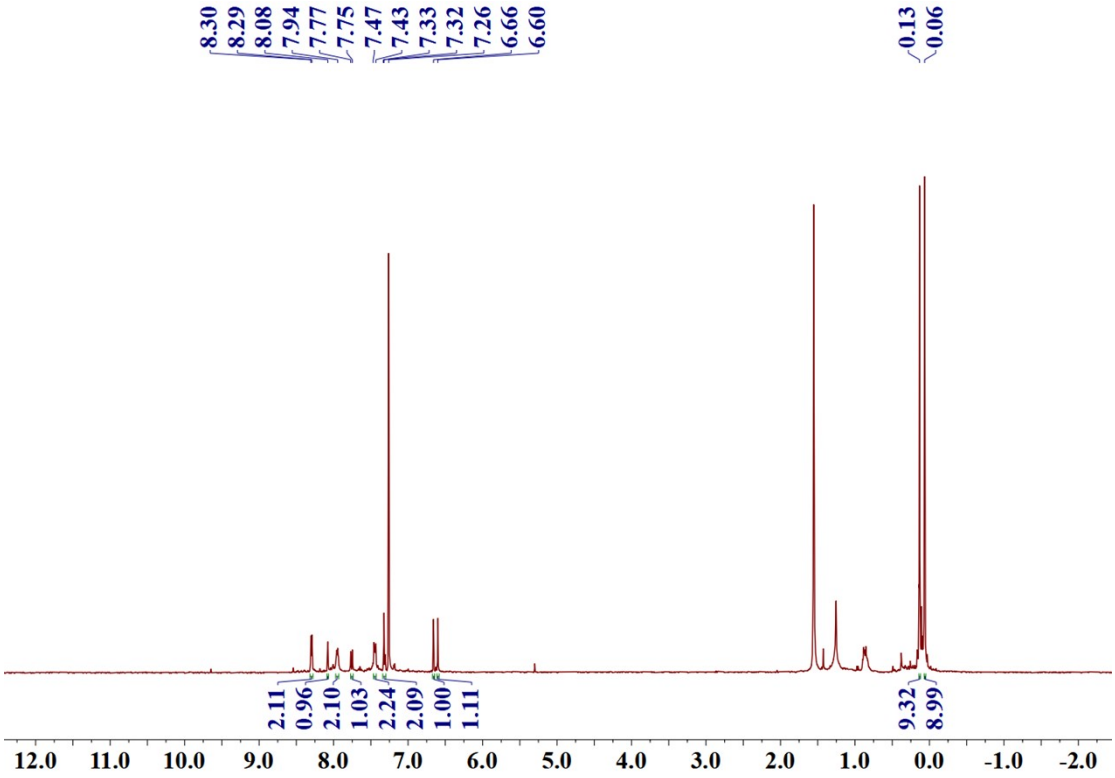

Figure S13. ^{1}H NMR (500 MHz, $CDCl_3$) spectrum of **BDTT-2An**.

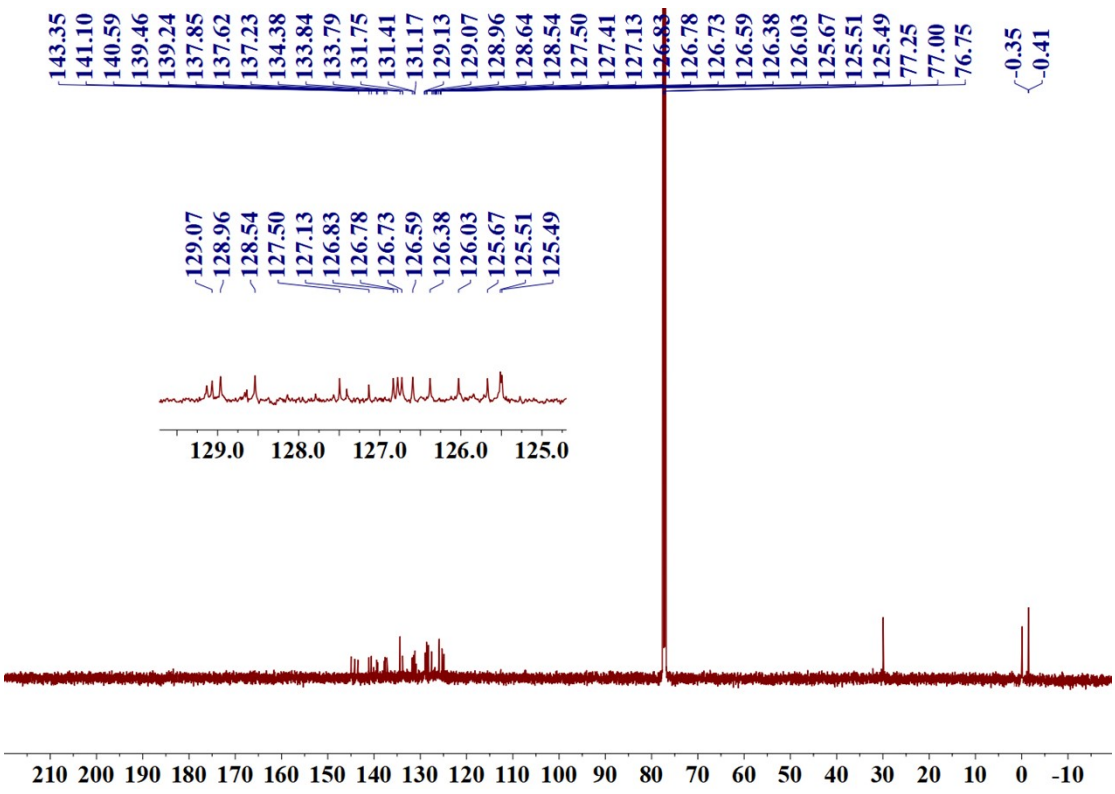

Figure S14. ^{13}C NMR (125 MHz, $CDCl_3$) spectra of **BDTT-2An**.

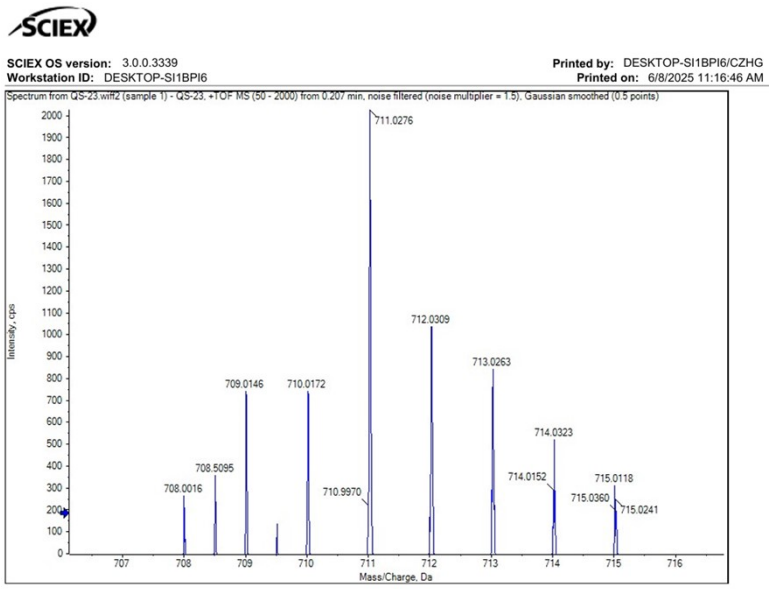

Figure S15. HRMS spectrum of **BDTT-2An**.

NMR and HRMS Spectra of BDTT-9An

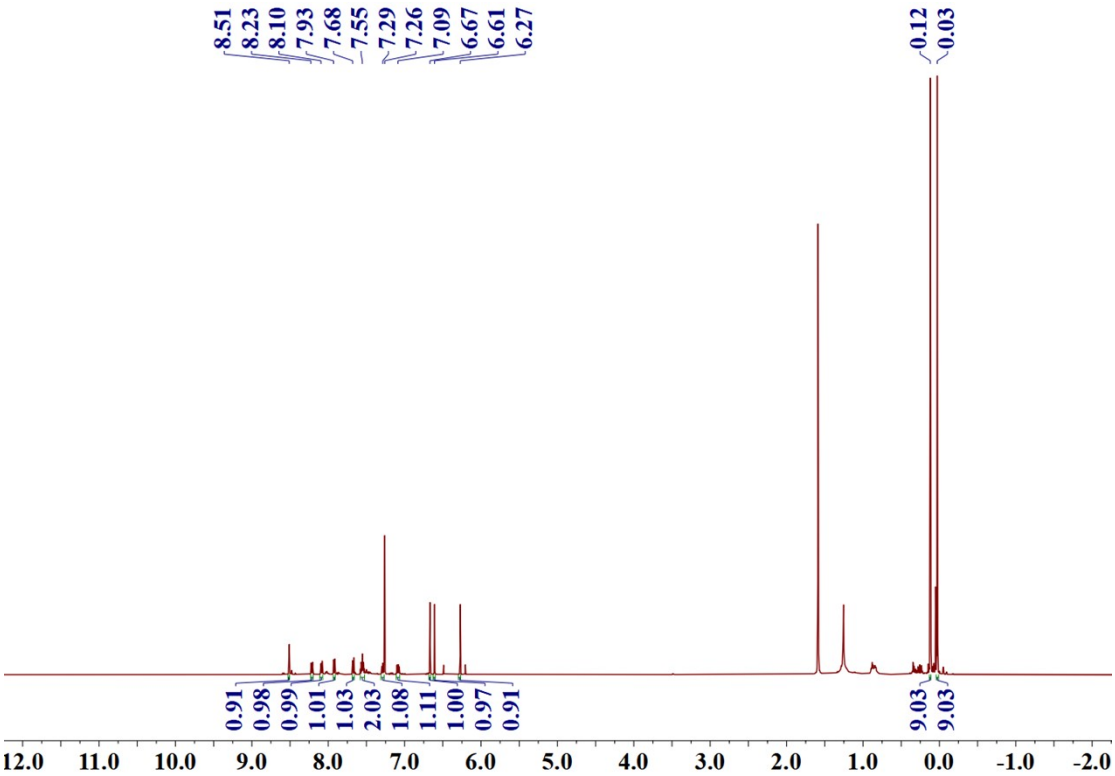

Figure S16. ^{1}H NMR (500 MHz, $CDCl_3$) spectrum of **BDTT-9An**.

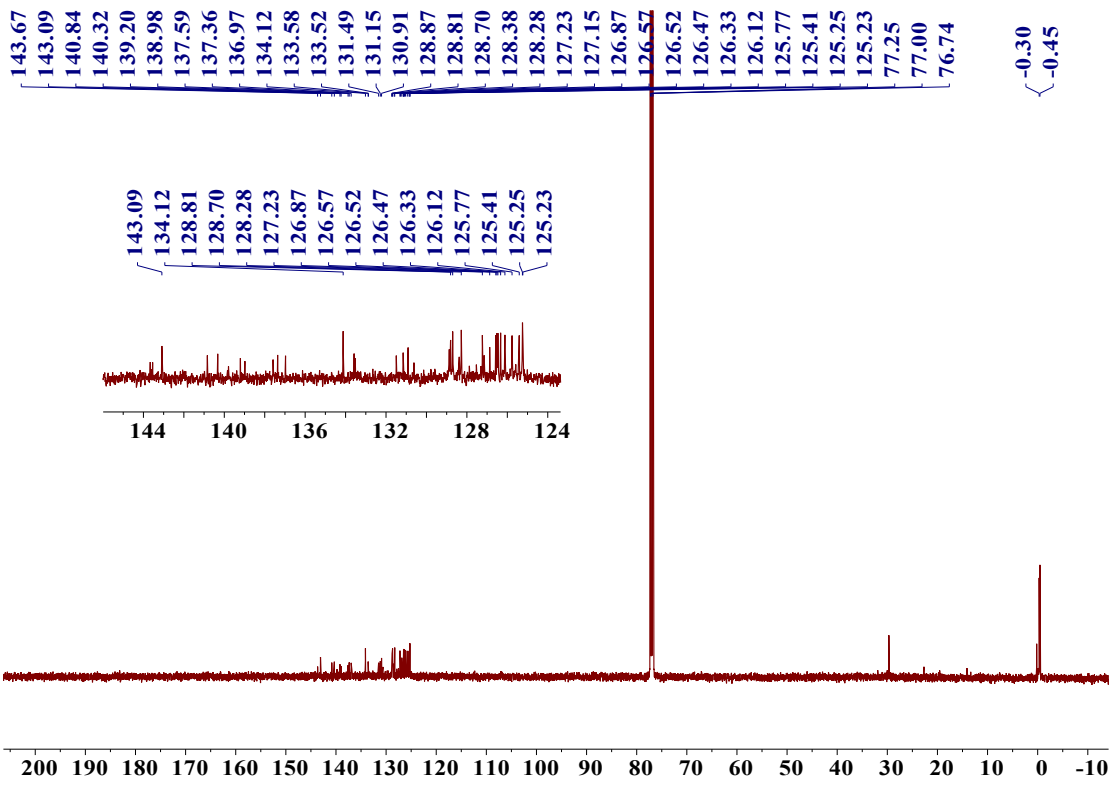

Figure S17. ^{13}C NMR (125 MHz, $CDCl_3$) spectra of **BDTT-9An**.

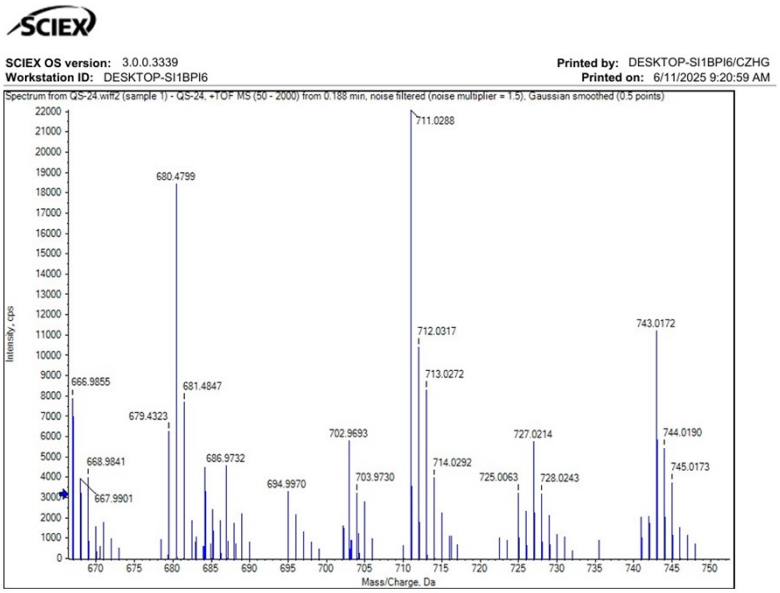

Figure S18. HRMS spectrum of **BDTT-9An**.

NMR and HRMS Spectra of BDTT-1Py

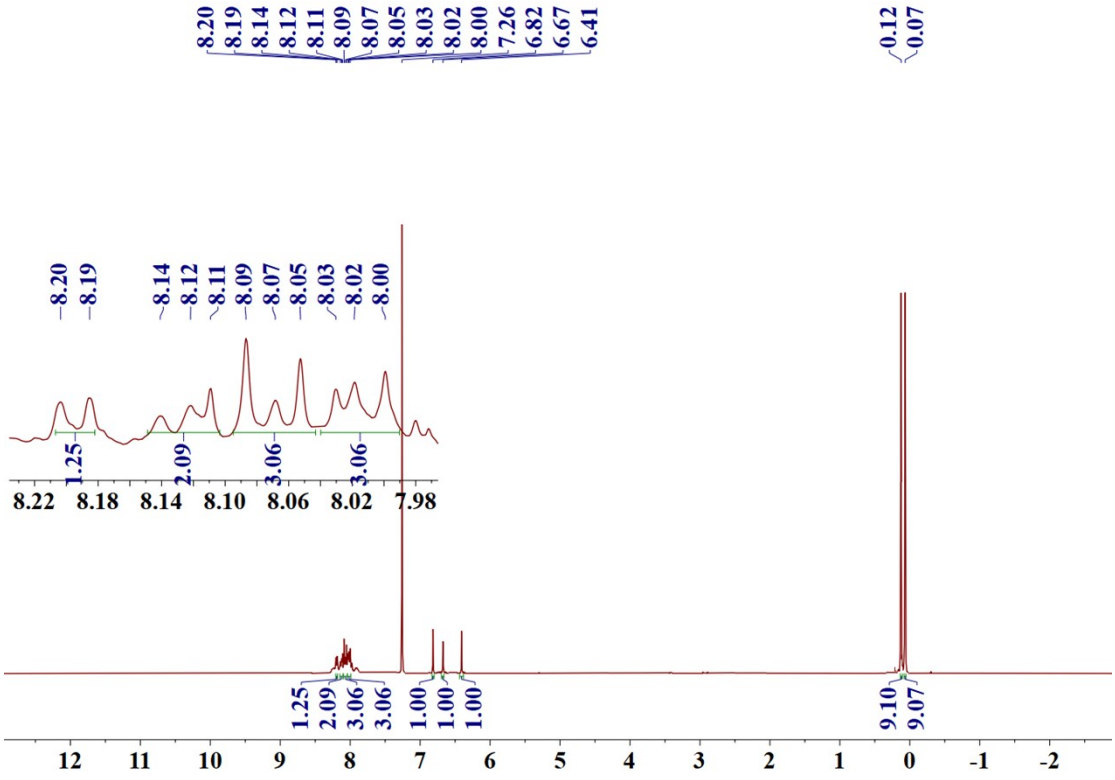

Figure S19. ^{1}H NMR (500 MHz, $CDCl_3$) spectra of **BDTT-1Py**.

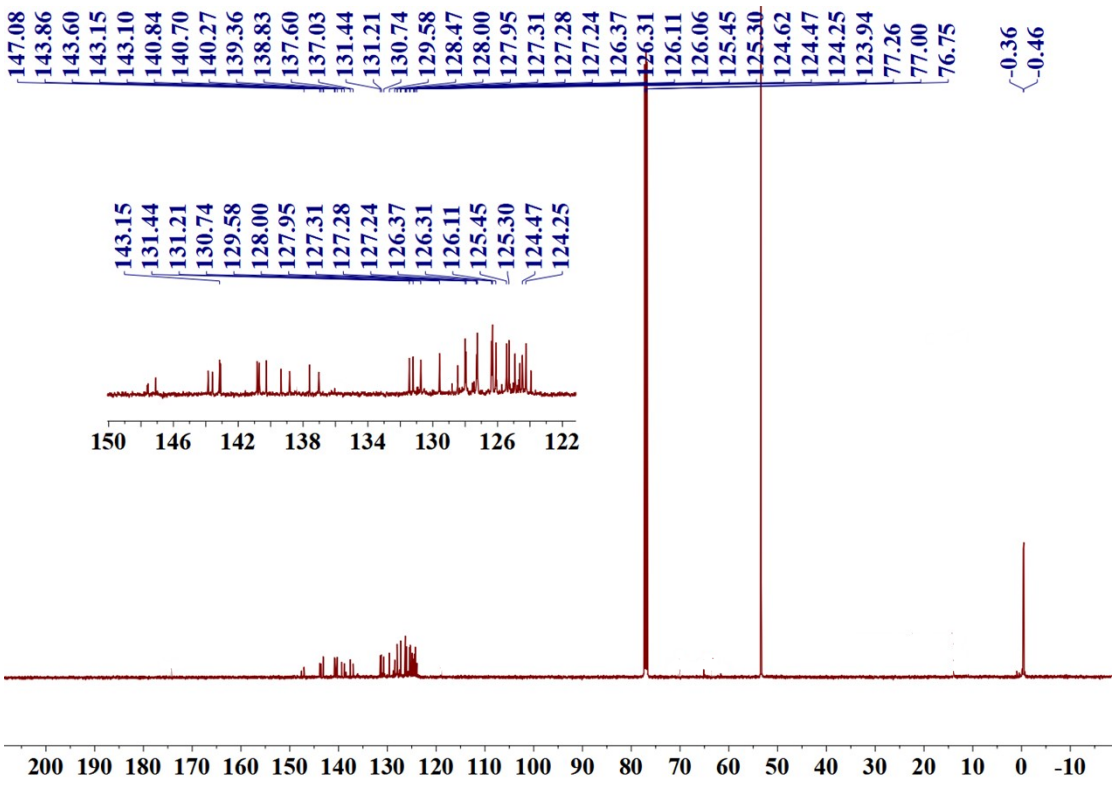

Figure S20. ^{13}C NMR (125 MHz, $CDCl_3$) spectra of **BDTT-1Py**.

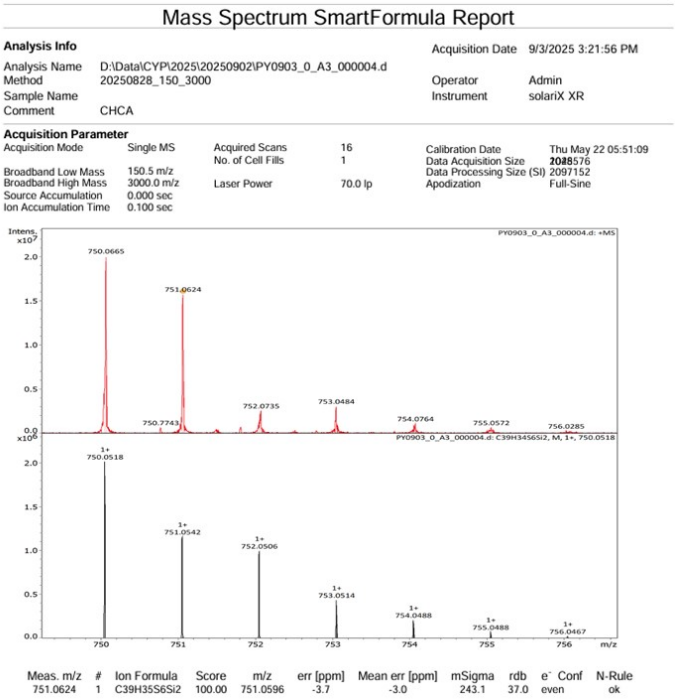

Figure S21. HRMS spectra of **BDTT-1Py**

3. Resolution, optical rotations, and racemization of BDTT-Ars

Resolution of BDTT-Me and optical rotations

The resolution of the **BDTT-Me** was carried out by chiral HPLC. The two enantiomers were obtained on a semipreparative scaled chiral column (CHIRALPAK-IB dimension: 10 mmϕ × 250 mmL); eluent: hexane; Injection information: concentration, 2.5 mg/mL and volume: 40 μL/injection. From the 3 mg scale of **BDTT-Me**, 1.0 mg (*ee* > 99%) of (−)-**BDTT-Me** and 1.1 mg (*ee* > 99%) of (+)-**BDTT-Me** were efficiently obtained. The optical rotations of (−)-**BDTT-Me**, $[\alpha]_D^{25} = -173°$ (c = 0.33 mg/mL in DCM) and (+)-**BDTT-Me**, $[\alpha]_D^{25} = +155°$ (c = 0.37 mg/mL in DCM) were observed.

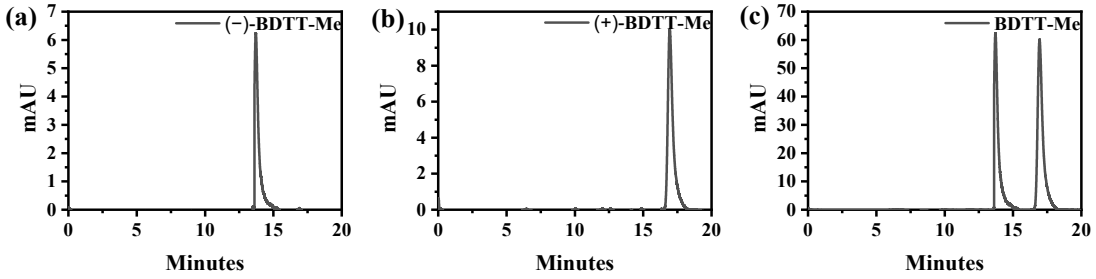

Figure S22. HPLC trace of (−)-**BDTT-Me** (a, *ee* > 99%), (+)-**BDTT-Me** (b, *ee* > 99%) and **BDTT-**

Me (c) at room temperature. Resolution of **BDTT-Me** by chiral HPLC monitored at 254 nm was performed with a CHIRALPAK IB column. Eluent: hexane, Flow Rate: 2.5 mL/min, Column: CHIRALPAK-IB.

Racemization of (+)-BDTT-Me

Racemization of (+)**-BDTT-Me** was carried out in CH_2Cl_2 by heating at different temperatures. The process was monitored from time to time by chiral HPLC (CHIRALPAK-IB) with hexane as eluent. The half-life of racemization of (+)**-BDTT-Me** is proposed as below:

	(+)**-BDTT-Me**	(+)**-BDTT-Me**
t = 0	C_0	0
t = t	C_t	$C_0 - C_t$

The racemization of (+)**-BDTT-Me** could be taken as first-order reaction, so

$$\ln(C_0/C_t) = kt$$

Here, C_0 is the concentration of (+)**-BDTT-Me** before heating, and C_t is the concentration of (+)**-BDTT-Me** after heating for time of t.

Because

$$ee = \frac{C_t - (C_0 - C_t)}{C_t + (C_0 - C_t)} = \frac{2C_t - C_0}{C_0} = 2\frac{C_t}{C_0} - 1$$

$$\Rightarrow \frac{C_t}{C_0} = \frac{ee + 1}{2}$$

So, we can obtain the formula as below:

$$ln\frac{C_0}{C_t} = \ln\frac{2}{ee + 1} = kt$$

$$\Rightarrow \ln\frac{ee + 1}{2} = -kt$$

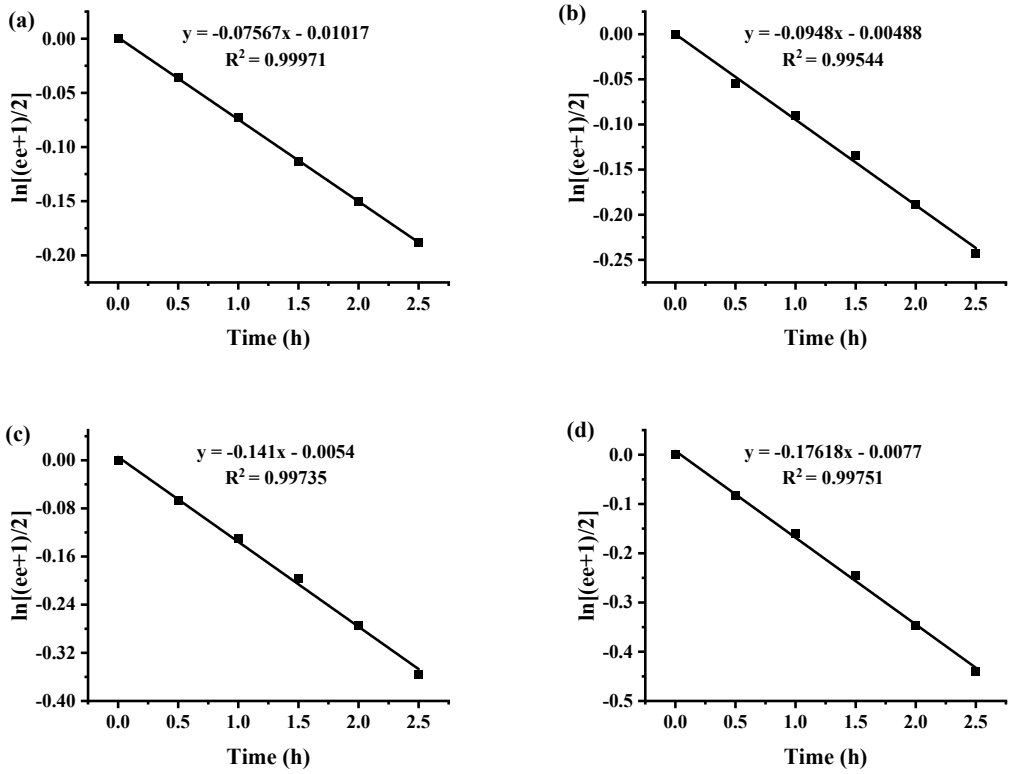

Figure S23. Time-dependent enantiomeric excess value decay profiles at (a) 40 °C, (b) 50 °C, (c) 60 °C, and (d) 70 °C, respectively.

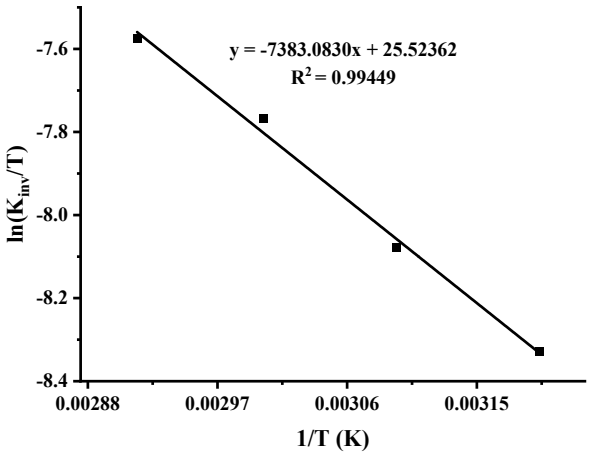

Figure S24. The half-life of (+)-**BDTT-Me** at different temperatures.

Table S1. The half-life of (+)-**BDTT-Me** at different temperatures.

T/°C	40	50	60	70
$t_{1/2}$/h	9.3	7.3	4.9	3.9

Table S2. The inversion barriers of (+)-**BDTT-Me** (R/S).

Compound	Δ*H*/kcal/mol	Δ*S*/J/k	Δ*G*/kcal/mol
(+)-**BDTT-Me**	14.68	14.67	13.72

Resolution of BDTT-Ph and optical rotations

The resolution of the **BDTT-Ph** was carried out by chiral HPLC. The two enantiomers were obtained on a semipreparative scaled chiral column (CHIRALPAK-IB dimension: 10 mmϕ × 250 mmL); eluent: hexane; Injection information: concentration, 2.5 mg/mL and volume: 100 μL/injection. From the 8 mg scale of **BDTT-Ph**, 1.9 mg (*ee* > 99%) of (−)-**BDTT-Ph** and 2.1 mg (*ee* > 99%) of (+)-**BDTT-Ph** were efficiently obtained. The optical rotations of (−)-**BDTT-Ph**, $[\alpha]_D^{25} = -675°$ (c = 0.30 mg/mL in DCM) and (+)-**BDTT-Ph**, $[\alpha]_D^{25} = +692°$ (c = 0.32 mg/mL in DCM) were observed.

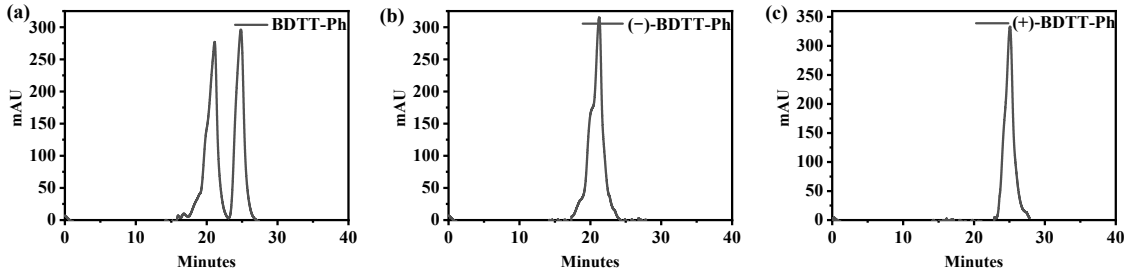

Figure S25. HPLC trace of **BDTT-Ph** (a), (−)-**BDTT-Ph** (b, *ee* > 99%) and (+)-**BDTT-Ph** (c, *ee* > 99%) at room temperature. Resolution of **BDTT-Ph** by chiral HPLC monitored at 254 nm was performed with a CHIRALPAK IB column. Eluent: hexane, Flow Rate: 2.5 mL/min, Column: CHIRALPAK-IB.

Racemization of (+)-BDTT-Ph

Racemization of (+)**-BDTT-Ph** was carried out in CH_2Cl_2 by heating at different temperatures. The process was monitored from time to time by chiral HPLC (CHIRALPAK-IB) with hexane as eluent. The half-life of (+)-**BDTT-Ph** was studied using the same method as for (+)**-BDTT-Me**:

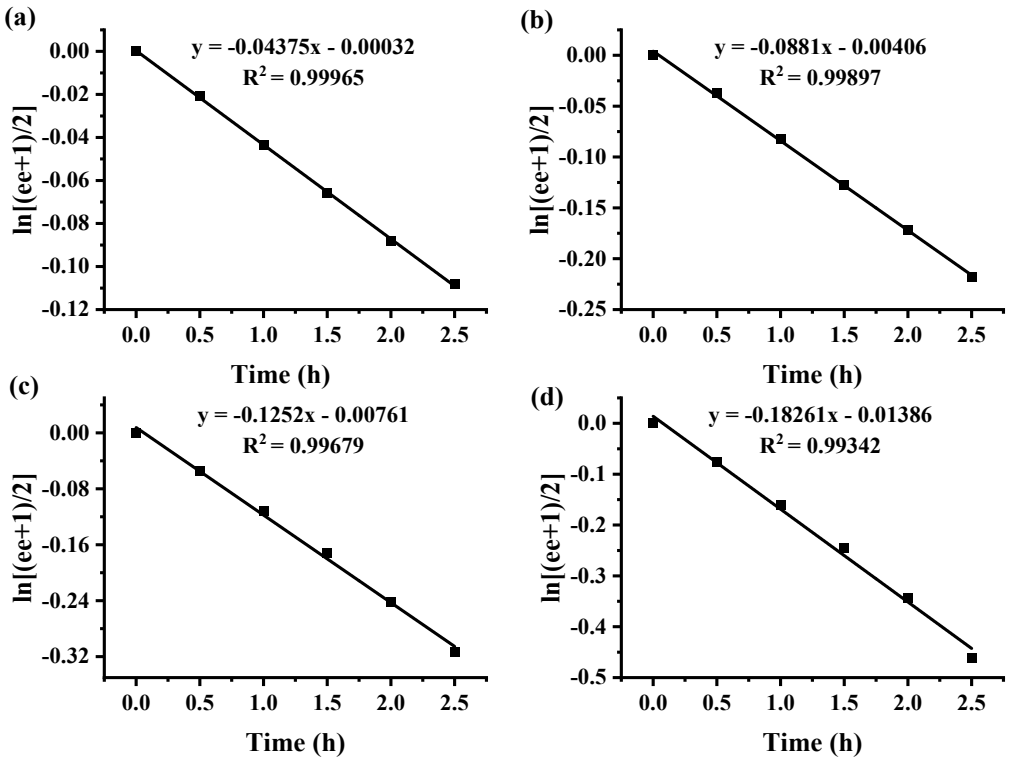

Figure S28. Time-dependent enantiomeric excess value decay profiles at (a) 50 °C, (b) 60 °C, (c) 70 °C, and (d) 80 °C, respectively.

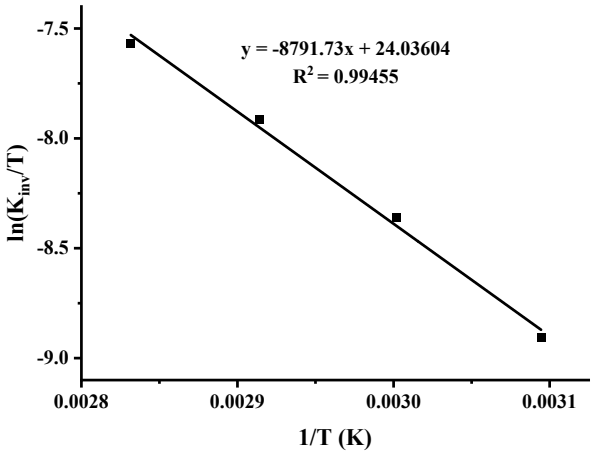

Figure S29. The half-life of (+)-**BDTT-Ph** at different temperatures.

Table S3. The half-life of (+)-**BDTT-Ph** at different temperatures.

T/°C	50	60	70	80
$t_{1/2}$/h	16.0	7.9	5.5	3.8

Table S4. The inversion barriers of (+)-**BDTT-Ph** (R/S).

Compound	Δ*H*/kcal/mol	Δ*S*/J/k	Δ*G*/kcal/mol
(+)-**BDTT-Ph**	17.47	2.31	17.32

Resolution of BDTT-1Np and optical rotations

The resolution of the **BDTT-1Np** was carried out by chiral HPLC. The two enantiomers were obtained on a semipreparative scaled chiral column (CHIRALPAK-IB dimension: 10 mmϕ × 250 mmL); eluent: hexane/dichloromethane (7/1, *v/v*); Injection information: concentration, 1 mg/mL and volume: 100 μL/injection. From the 4 mg scale of **BDTT-1Np**, 1.5 mg (*ee* > 99%) of (+)-**BDTT-1Np** and 1.7 mg (*ee* > 99%) of (−)-**BDTT-1Np** were efficiently obtained. The optical rotations of (−)-**BDTT-1Np**, $[\alpha]_D^{25}$ = − 897º (c = 0.34 mg/mL in DCM) and (+)-**BDTT-1Np**, $[\alpha]_D^{25}$ = + 842º (c = 0.30 mg/mL in DCM) were observed.

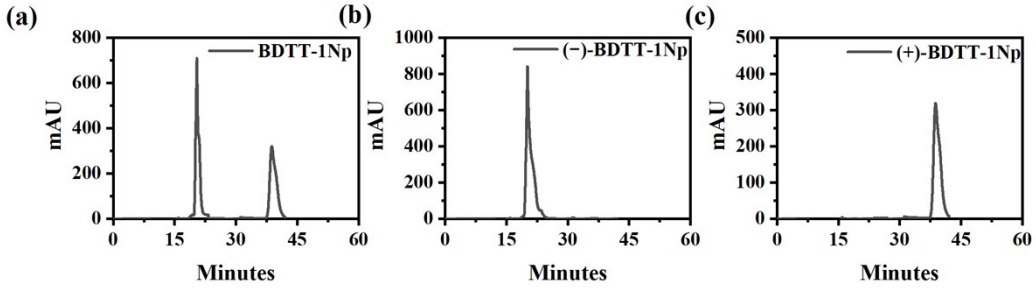

Figure S30. HPLC trace of **BDTT-1Np** (a), (−)-**BDTT-1Np** (b, *ee* > 99%) and (+)-**BDTT-1Np** (c, *ee* > 99%) at room temperature. Resolution of **BDTT-1Np** by chiral HPLC monitored at 254 nm was performed with a CHIRALPAK IB column. Eluent: hexane/dichloromethane (7/1, *v/v*), Flow Rate: 2.5 mL/min, Column: CHIRALPAK-IB.

Racemization of (+)-BDTT-1Np

Racemization of (+)-**BDTT-1Np** was carried out in CH_2Cl_2 by heating at different temperatures. The process was monitored from time to time by chiral HPLC (CHIRALPAK-IB)

with hexane /dichloromethane (7/1, *v/v*) as eluent. The half-life of (+)-**BDTT-1Np** was studied using the same method as for (+)-**BDTT-Me**:

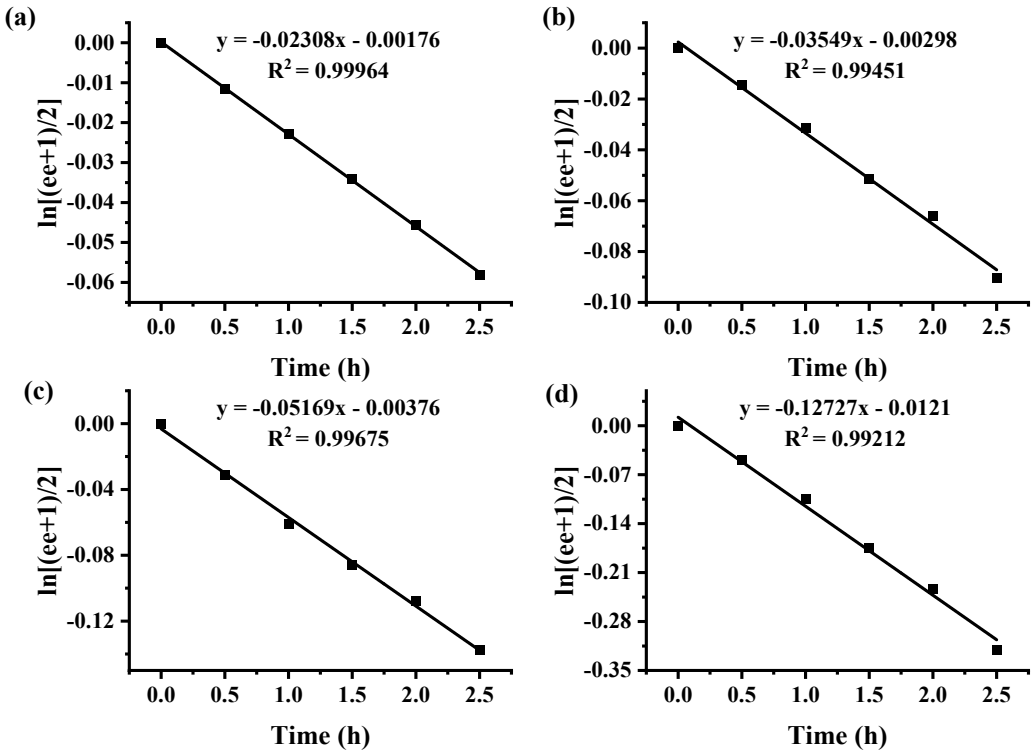

Figure S31. Time-dependent enantiomeric excess value decay profiles at (a) 60 °C, (b) 70 °C, (c) 80 °C and (d) 90 °C, respectively.

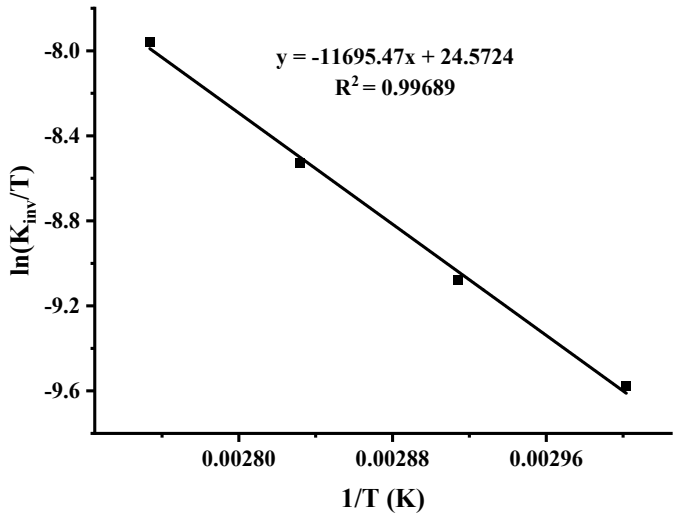

Figure S32. The half-life of (+)-**BDTT-1Np** at different temperatures.

Table S5. The half-life of (+)-**BDTT-1Np** at different temperatures.

T/°C	60	70	80	90
$t_{1/2}$/h	30.0	20.0	13.4	5.5

Table S6. The inversion barriers of (+)-**BDTT-1Np** (R/S).

Compound	Δ*H*/kcal/mol	Δ*S*/J/k	Δ*G*/kcal/mol
(+)-**BDTT-1Np**	23.24	6.77	22.8

Resolution of BDTT-2Np and optical rotations

The resolution of the **BDTT-2Np** was carried out by chiral HPLC. The two enantiomers were obtained on a semipreparative scaled chiral column (CHIRALPAK-IB dimension: 10 mmϕ × 250 mmL); eluent: hexane/dichloromethane (6/1, *v/v*); Injection information: concentration, 1mg/mL and volume: 130 μL/injection. From the 3.7 mg scale of **BDTT-2Np**, 1.0 mg (*ee* > 99%) of (+)-**BDTT-2Np** and 1.1 mg (*ee* > 99%) of (−)-**BDTT-2Np** were efficiently obtained. The optical rotations of (−)-**BDTT-2Np**, $[\alpha]_D^{25}$ = − 770° (c = 0.32 mg/mL in DCM) and (+)-**BDTT-2Np**, $[\alpha]_D^{25}$ = + 743° (c = 0.32 mg/mL in DCM) were observed.

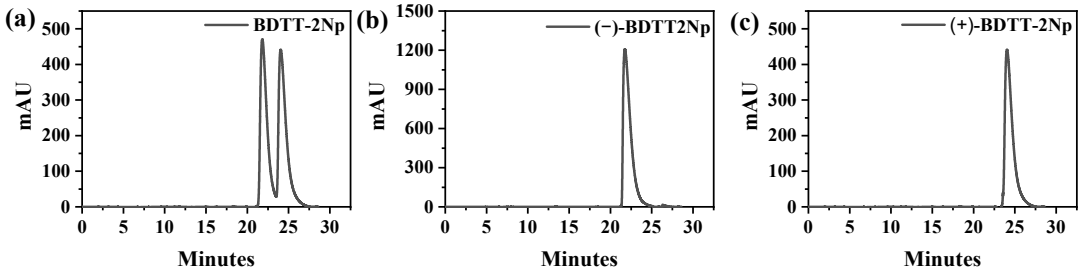

Figure S32. HPLC trace of **BDTT-2Np** (a), (−)-**BDTT-2Np** (b, *ee* > 99%) and (+)-**BDTT-2Np** (c, *ee* > 99%) at room temperature. Resolution of **BDTT-2Np** by chiral HPLC monitored at 254 nm was performed with a CHIRALPAK IB column. Eluent: hexane/dichloromethane (6/1, *v/v*), Flow Rate: 2.5 mL/min, Column: CHIRALPAK-IB.

Racemization of (+)-BDTT-2Np

Racemization of (+)-**BDTT-2Np** was carried out in CH_2Cl_2 by heating at different temperatures. The process was monitored from time to time by chiral HPLC (CHIRALPAK-IB) with hexane/dichloromethane (6/1, *v/v*) as eluent. The half-life of (+)-**BDTT-2Np** was studied using the same method as for (+)**-BDTT-Me**:

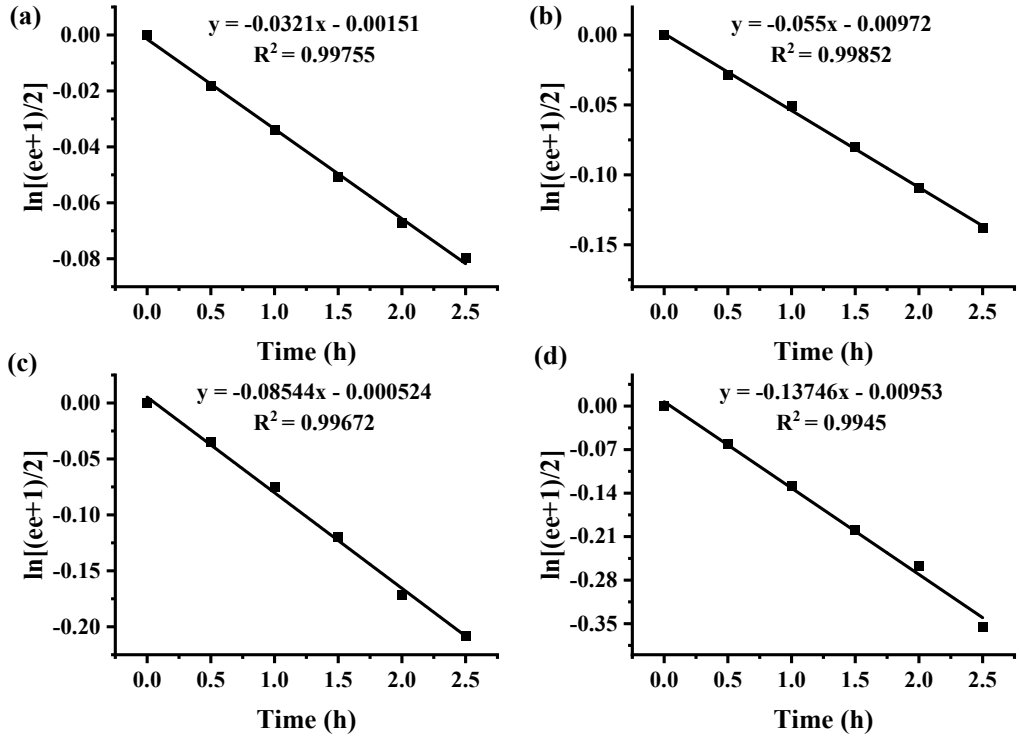

Figure S33. Time-dependent enantiomeric excess value decay profiles at (a) 60 °C, (b) 70 °C, (c) 80 °C, and (d) 90 °C, respectively.

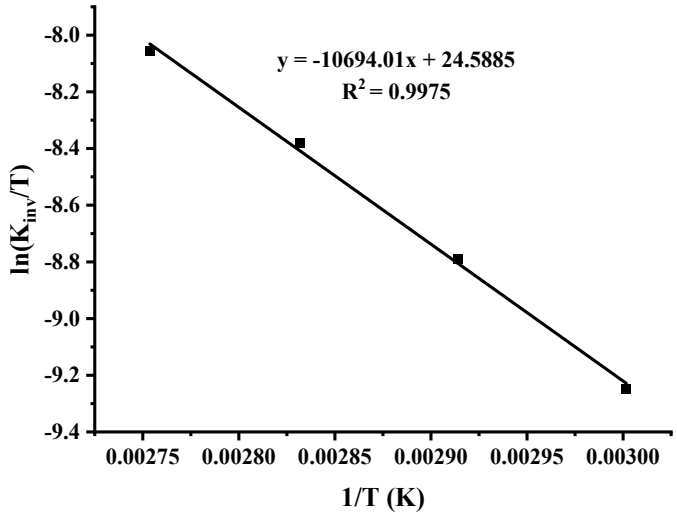

Figure S34. The half-life of (+)-**BDTT-2Np** at different temperatures.

Table S7. The half-life of (+)-**BDTT-2Np** at different temperatures.

T/°C	60	70	80	90
$t_{1/2}$/h	21.6	12.6	8.1	5.0

TableS8. The inversion barriers of (−)-**BDTT-2Np** (R/S).

Compound	Δ*H*/kcal/mol	Δ*S*/J/k	Δ*G*/kcal/mol
(−)-**BDTT-2Np**	21.26	6.9	20.9

Resolution of BDTT-2An and optical rotations

The resolution of the **BDTT-2An** was carried out by chiral HPLC. The two enantiomers were obtained on a semipreparative scaled chiral column (CHIRALPAK-IB dimension: 10 mmϕ × 250 mm); eluent: hexane/dichloromethane (5/1, *v/v*); Injection information: concentration, 2 mg/mL and volume: 150 μL/injection. From the 4.2 mg scale of **BDTT-2An**, 0.9 mg (*ee* > 99%) of (−)-**BDTT-2An** and 1.1 mg (*ee* > 99%) of (+)-**BDTT-2An** were efficiently obtained. The optical rotations of (−)-**BDTT-2An**, $[\alpha]_D^{25}$ = − 1036° (c = 0.350 mg/mL in DCM) and (+)-**BDTT-2An**, $[\alpha]_D^{25}$ = + 1002° (c = 0.37 mg/mL in DCM) were observed.

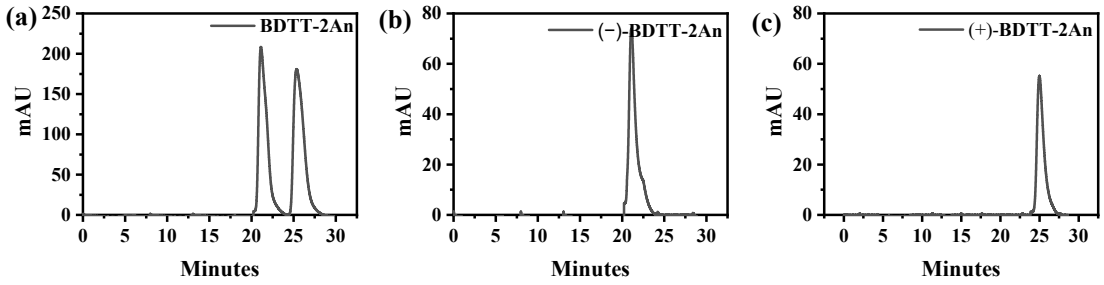

Figure S35. HPLC trace of **BDTT-2An** (a), (−)-**BDTT-2An** (b, *ee* > 99%) and (+)-**BDTT-2An** (c, *ee* > 99%) at room temperature. Resolution of **BDTT-2An** by chiral HPLC monitored at 254 nm was performed with a CHIRALPAK-IB column. Eluent: hexane/dichloromethane (5/1, *v/v*), Flow Rate: 2.5 mL/min, Column: CHIRALPAK-IB.

Racemization of (+)-BDTT-2An

Racemization of (+)-**BDTT-2An** was carried out in CH_2Cl_2 by heating at different temperatures. The process was monitored from time to time by chiral HPLC (CHIRALPAK-IB) with hexane/dichloromethane (5/1, *v/v*) as eluent. The half-life of (+)-**BDTT-2An** was studied using the same method as for (+)-**BDTT-Me**:

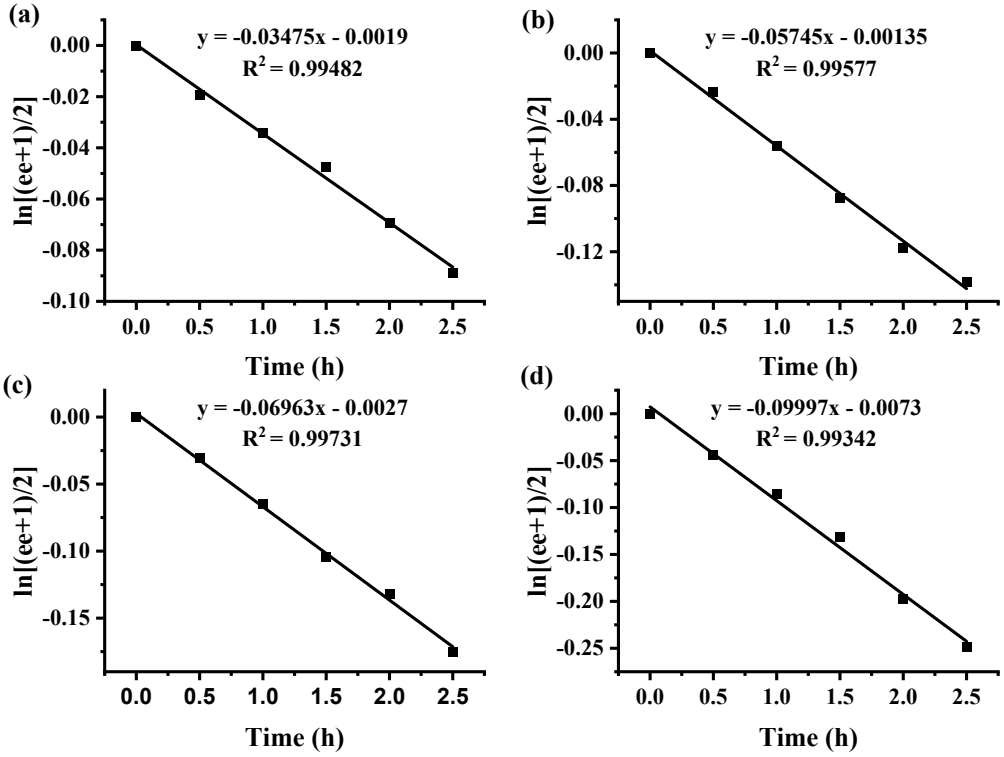

Figure S36. Time-dependent enantiomeric excess value decay profiles at (a) 100 °C, (b) 110 °C, (c) 120 °C, and (d) 130 °C, respectively.

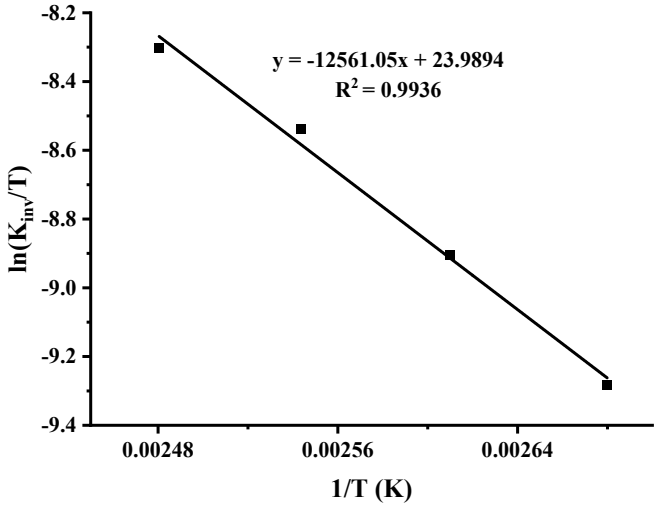

Figure S37. The half-life of (+)-**BDTT-2An** at different temperatures.

Table S9. The half-life of (+)-**BDTT-2An** at different temperatures.

T/°C	100	110e	120	130
$t_{1/2}$/h	20.0	12.2	9.9	7.0

Table S10. The inversion barriers of (+)-**BDTT-2An** (*R*/*S*).

Compound	Δ*H*/kcal/mol	Δ*S*/J/k	Δ*G*/kcal/mol
(+)-**BDTT-2An**	24.96	1.92	24.83

Resolution of BDTT-9An and optical rotations

The resolution of the **BDTT-9An** was carried out by chiral HPLC. The two enantiomers were obtained on a semipreparative scaled chiral column (CHIRALPAK-IB dimension: 10 mmϕ × 250 mmL); eluent: hexane/dichloromethane (95/5, *v/v*); Injection information: concentration, 2.5 mg/mL and volume: 100 μL/injection. From the 6.2 mg scale of **BDTT-9An**, 1.0 mg (*ee* > 99%) of (−)-**BDTT-9An** and 1.3 mg (*ee* > 99%) of (+)-**BDTT-9An** were efficiently obtained. The optical rotations of (−)-**BDTT-9An**, $[\alpha]_D^{25}$ = − 1186° (c = 0.35 mg/mL in DCM) and (+)-**BDTT-9An**, $[\alpha]_D^{25}$ = + 1108° (c = 0.35 mg/mL in DCM) were observed.

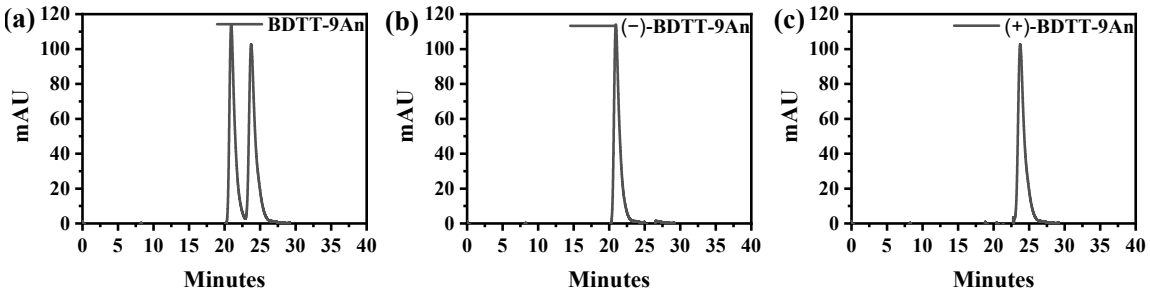

Figure S38. HPLC trace of **BDTT-9An** (a), (−)-**BDTT-9An** (b, *ee* > 99%) and (+)-**BDTT-9An** (c, *ee* > 99%) at room temperature. Resolution of **BDTT-9An** by chiral HPLC monitored at 254 nm was performed with a CHIRALPAK IB column. Eluent: hexane /dichloromethane (95/5, *v/v*), Flow Rate: 2.5 mL/min, Column: CHIRALPAK-IB.

Racemization of (+)-BDTT-9An

Racemization of (+)-**BDTT-9An** was carried out in CH_2Cl_2 by heating at different temperatures. The process was monitored from time to time by chiral HPLC (CHIRALPAK-IB) with hexane/dichloromethane (95/5, *v/v*) as eluent. The half-life of (+)-**BDTT-9An** was studied using the same method as for (+)-**BDTT-Me**:

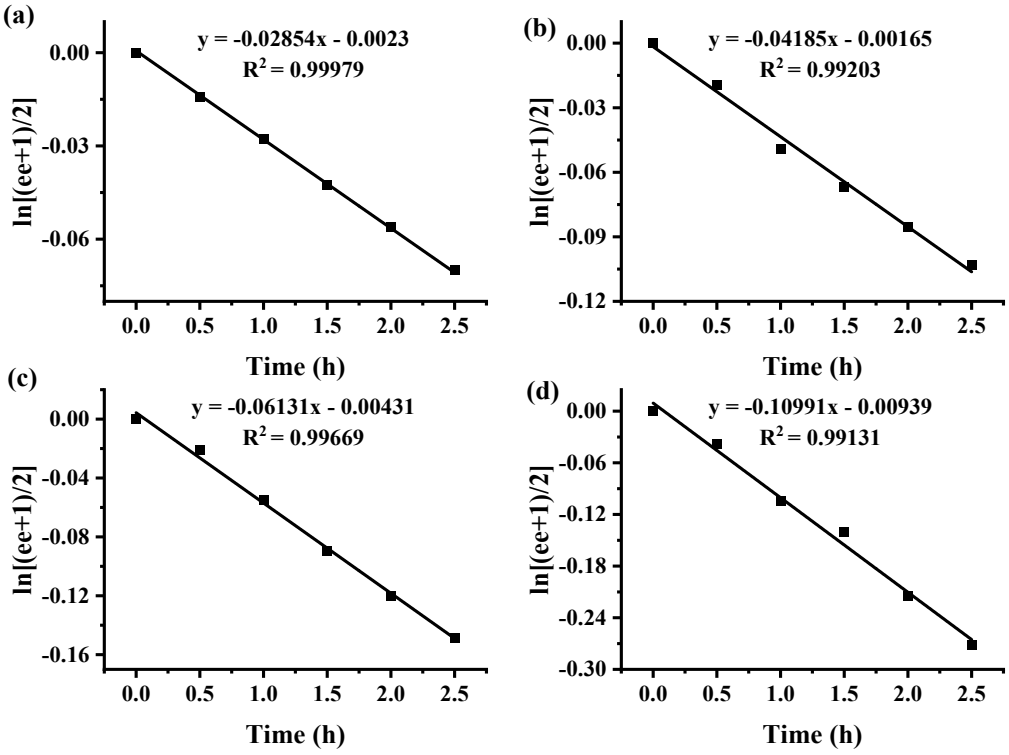

Figure S39. Time-dependent enantiomeric excess value decay profiles at (a) 120 °C, (b) 130 °C, (c) 140 °C, and (d) 150 °C, respectively.

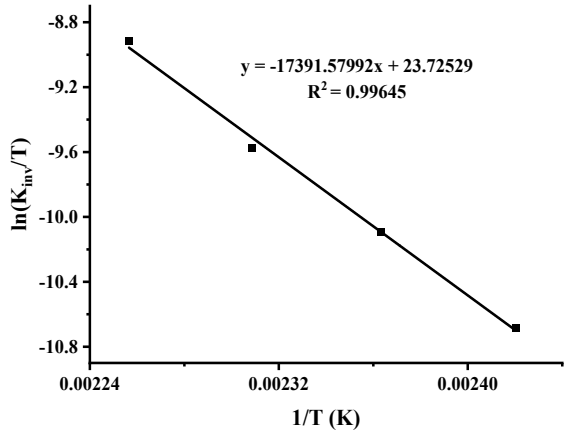

Figure S40. The half-life of (+)-**BDTT-9An** at different temperatures.

Table S11. The half-life of (+)-**BDTT-9An** at different temperatures.

T/°C	120	130	140	150
$t_{1/2}$/h	24.8	16.6	10.3	6.3

Table S12. The inversion barriers of (+)-**BDTT-9An** (R/S).

Compound	Δ*H*/kcal/mol	Δ*S*/J/k	Δ*G*/kcal/mol
(+)-**BDTT-9An**	30.26	8.18	29.73

Resolution of BDTT-1Py and optical rotations

The resolution of the **BDTT-1Py** was carried out by chiral HPLC. The two enantiomers were obtained on a semipreparative scaled chiral column (CHIRALPAK-IB dimension: 10 mmϕ × 250 mmL); eluent: hexane/dichloromethane (3/1, *v/v*); Injection information: concentration, 2.5 mg/mL and volume: 100 μL/injection. From the 5.0 mg scale of **BDTT-1Py**, 1.2 mg (*ee* > 99%) of (−)-**BDTT-1Py** and 1.5 mg (*ee* > 99%) of (+)-**BDTT-1Py** were efficiently obtained. The optical rotations of (−)-**BDTT-1Py**, $[\alpha]_D^{25}$ = − 1205° (c = 0.38 mg/mL in DCM) and (+)-**BDTT-1Py**, $[\alpha]_D^{25}$ = + 1242° (c = 0.38 mg/mL in DCM) were observed.

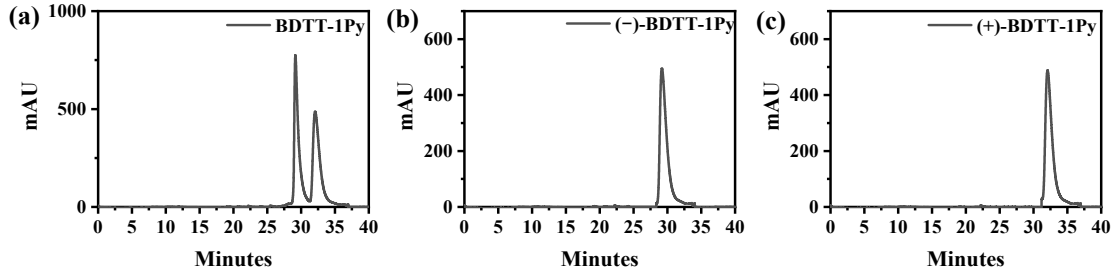

Figure S41. HPLC trace of **BDTT-1Py** (a), (−)-**BDTT-1Py** (b, *ee* > 99%) and (+)-**BDTT-1Py** (c, *ee* > 99%) at room temperature. Resolution of **BDTT-1Py** by chiral HPLC monitored at 254 nm was performed with a CHIRALPAK IB column. Eluent: hexane /dichloromethane (3/1, *v/v*), Flow Rate: 2.5 mL/min, Column: CHIRALPAK-IB.

Racemization of (+)-BDTT-1Py

Racemization of (+)-**BDTT-1Py** was carried out in DCM by heating at different temperatures. The process was monitored from time to time by chiral HPLC (CHIRALPAK-IB) with hexane/dichloromethane (3/1, *v/v*) as eluent. The half-life of (+)-**BDTT-1Py** was studied using the same method as for (+)-**BDTT-Me**:

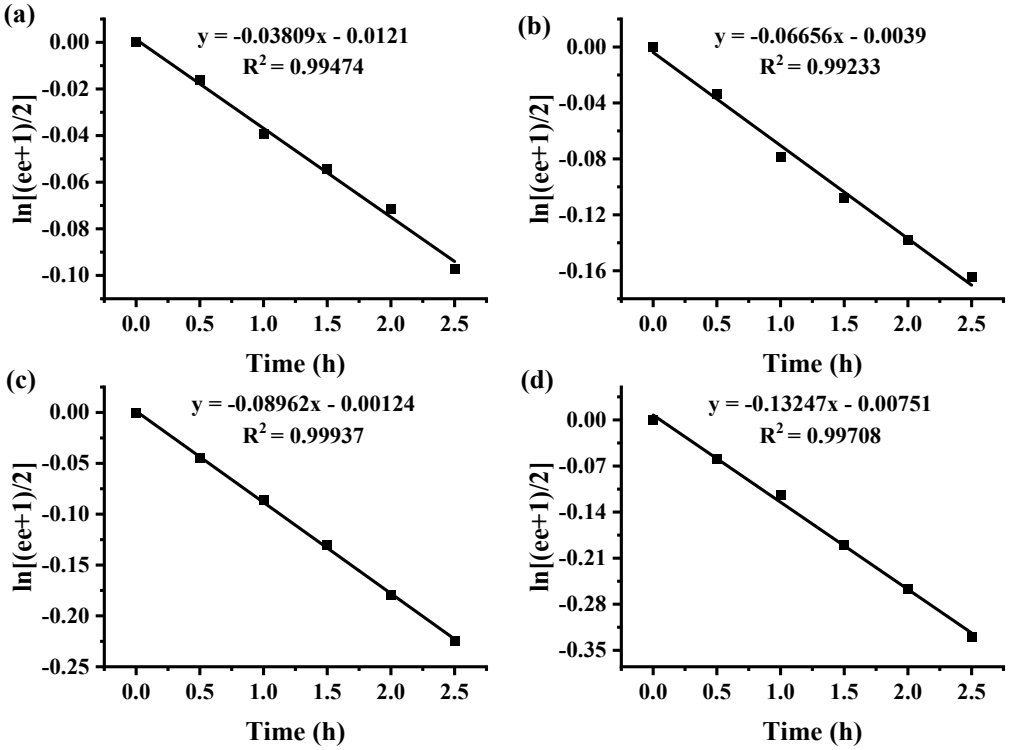

Figure S42. Time-dependent enantiomeric excess value decay profiles at (a) 100 °C, (b) 110 °C, (c) 120 °C, and (d) 130 °C, respectively.

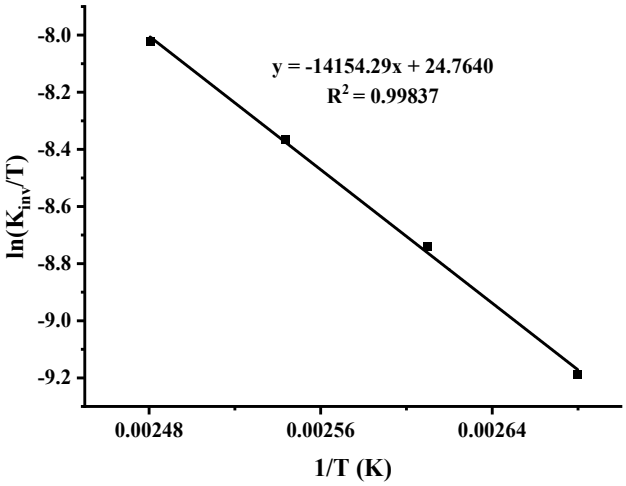

Figure S43. The half-life of (+)-**BDTT-1Py** at different temperatures.

Table S13. The half-life of (+)-**BDTT-1Py** at different temperatures.

T/°C	100	110	120	130
$t_{1/2}$/h	18.2	10.4	7.7	5.2

Table S14. The inversion barriers of (+)-**BDTT-1Py** (R/S).

Compound	Δ*H*/kcal/mol	Δ*S*/J/k	Δ*G*/kcal/mol
(+)-**BDTT-1Py**	28.13	8.36	27.58

4. Optical and electrochemical data of BDTT-Ars.

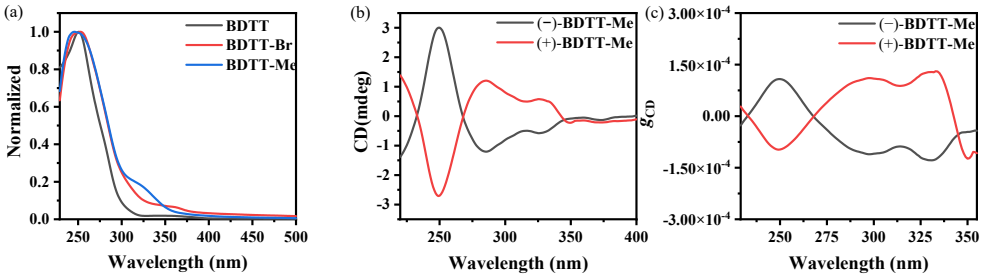

Figure S44. (a) Absorption spectra of **BDTT**，**BDTT-Br** and **BDTT-Me**; (b) CD spectra of **BDTT-Me** in DCM, [C] = 1.0 × 10^{-4} M and (c) Absorption dissymmetry factor g_{abs} corresponded CD spectra of (−)-**BDTT-Me** and (+)-**BDTT-Me** at room temperature.

Table S15. Optical and electrochemical data of **BDTT-Ar**s.

Compound	λ_{abs} (nm)[a]	λ_{FL} (nm)[a]	λ_{PL} (nm)[b]	Φ_F /%[c]	τ_{FL} (ns)[a]	τ_{PL} (ms)[b]	E_g^{opt} (eV)	HOMO (eV)[d]	LUMO (eV)[d]	k_r (10^6 S^{-1})[e]	k_{nr} (10^9 S^{-1})[f]
BDTT-Me	246, 317	--	--	--	--	--	3.86	-5.74	-1.88	--	--
BDTT-Ph	244, 314	400	504, 534	0.03/0.05[f]	0.87	10	3.70	-5.70	-2.00	0.34	1.15
BDTT-1Np	248, 319	403	506, 542	0.06/0.11[f]	2.1	8	3.86	-5.68	-2.03	0.29	0.47
BDTT-2Np	244, 328	408	512, 548	0.32/0.58[f]	2.7	4	3.70	-5.62	-2.25	1.20	0.37
BDTT-2An	259, 329	445	528, 552	0.47/2.94[f]	6.3	110	3.65	-5.53	-2.46	0.75	0.16
BDTT-9An	258, 380	358	544	0.19/2.72[f]	1.7	26	3.37	-5.50	-2.40	1.10	0.59
BDTT-1Py	242, 352	446	614, 672	0.59/3.16[f]	7.2	75	3.07	-5.45	-2.39	0.82	0.14

[a]In DCM solution at RT (1×10^{-5} M); [b]In 2-MTHF solution at 77 K (1×10^{-5} M); [c]Relative fluorescence quantum yield using quinine sulphate (Φ_F = 0.55, 1×10^{-5} M in 0.5 M H_2SO_4) as a standard; [d]CV measured in 0.1 M TBAF/ DCM at a scan rate of 100 mV/s, [C] = 1×10^{-3} M, vs Fc/Fc^+. $E_{HOMO} = -[E_{ox} - E_{(FC/FC^+)} + 4.8]$ eV. $E_{LUMO} = E_g + E_{HOMO}$. [e]Radiative decay rate constants calculated by $\Phi_F = k_r \times \tau_F$. [f]Nonradiative rate constants calculated by $k_r + k_{nr} = \tau_F^{-1}$. [f]The fluorescence quantum yields in solid states, Edinburgh FLS1000.

Cyclic voltammetries of BDTT-Ars

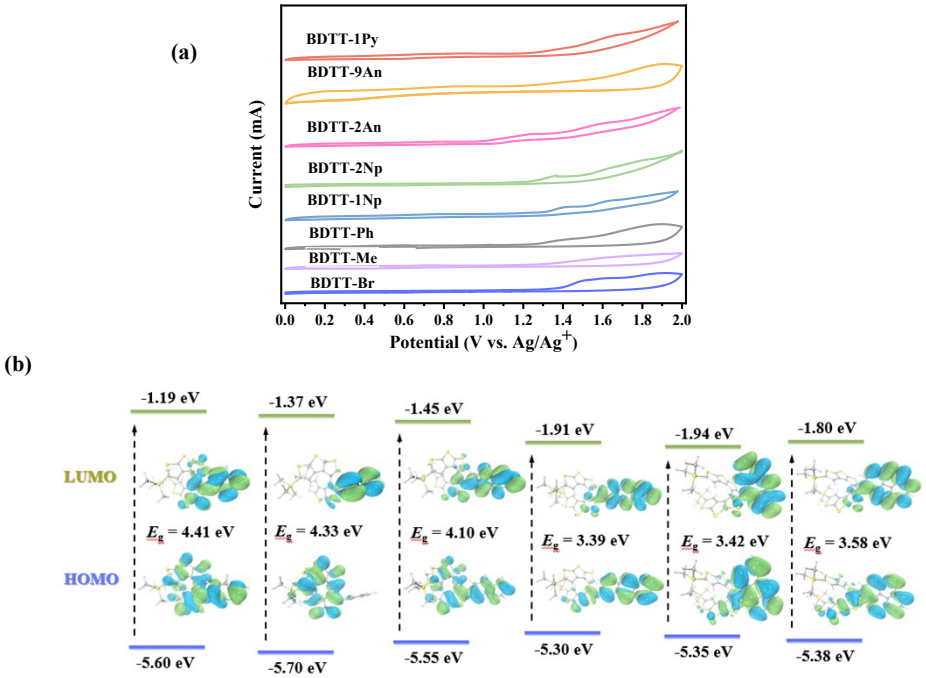

Figure S45. (a) Cyclic voltammogram (classical presentation) of **BDTT-Ar**s in DCM ([C] = 1 ×

10^{-3} M, supporting electrolyte: [nBu$_4$N][PF$_6$] (0.1 M), scan rate: 100 mV s^{-1}, room temperature).

(b) Visualizations of HOMO and LUMO distributions (B3LYP/6-31G*) for **BDTT-Ar**s.

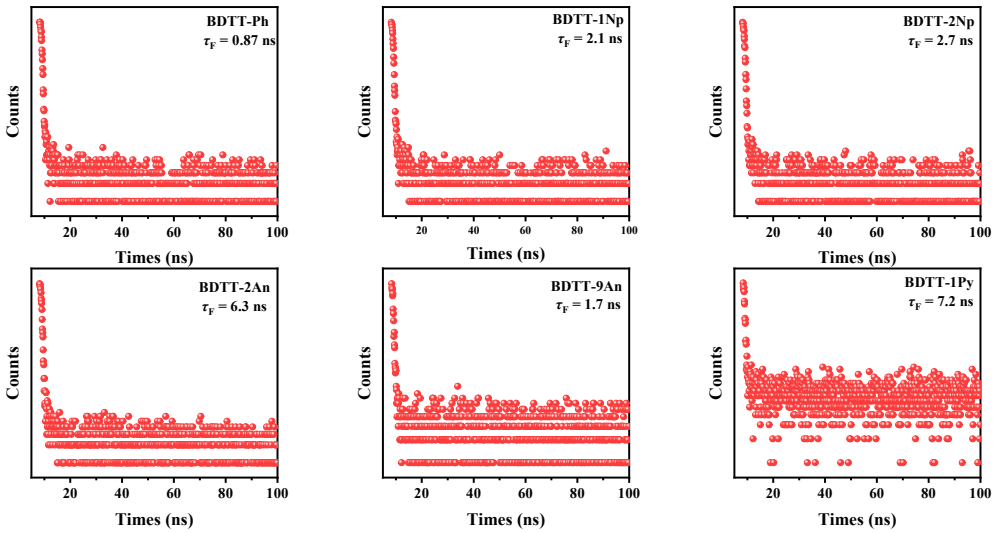

Figure S46. Time-resolved fluorescence decay of **BDTT-Ar**s in DCM at room temperature.

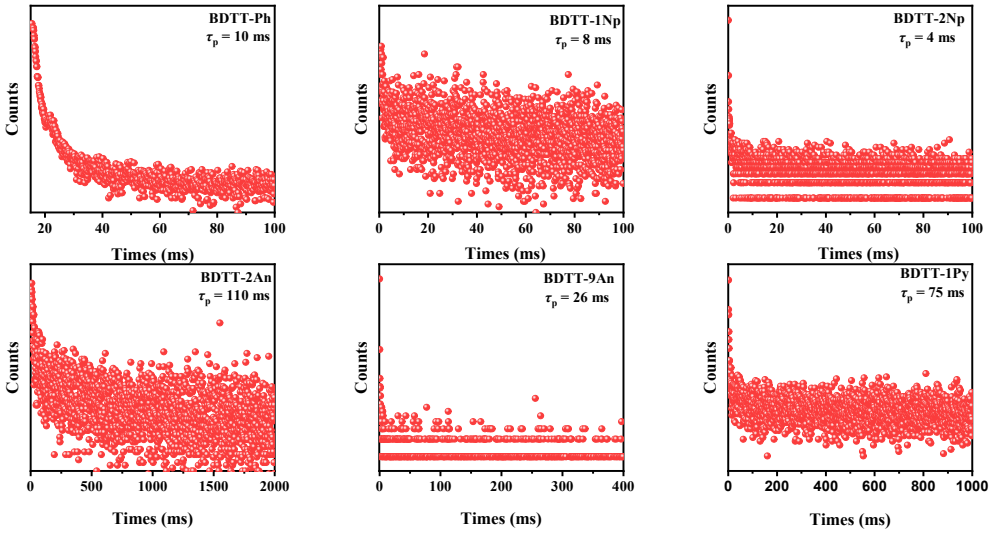

Figure S47. Phosphorescence transient decay spectra of **BDTT-Ar**s in 2-MTHF at 77 K.

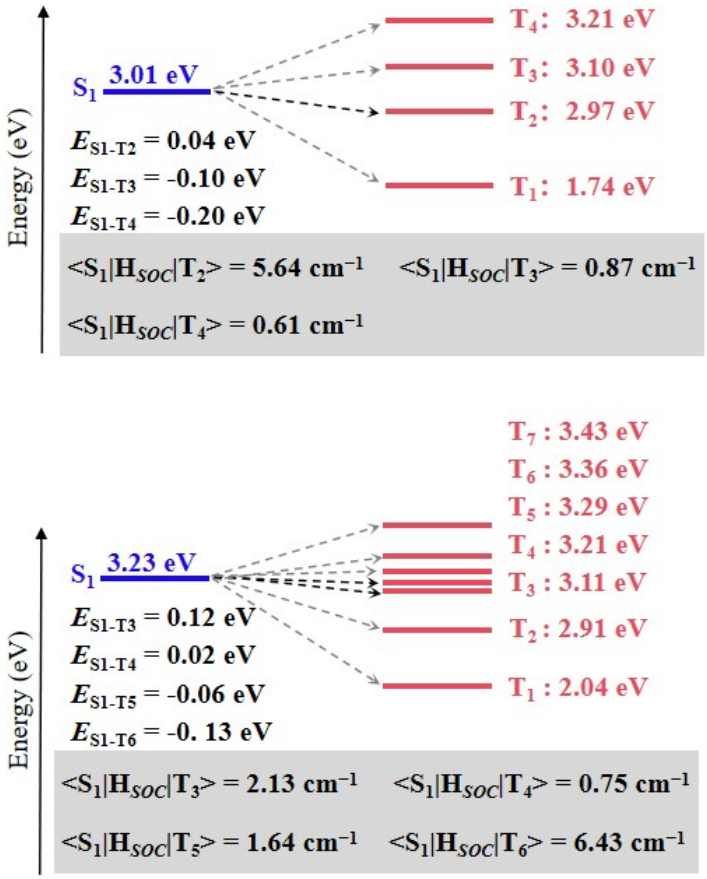

Figure S48. The fluorescence quantum Theoretical calculations of ISC channels, SOC matrix elements, and frontier molecular orbitals of **BDTT-9An** (up) and **BDTT-1Py** (down).

5. References

S1. Suffert, J. Simple Direct Titration of Organolithium Reagents Using *N*-Pivaloyl-*o*-toluidine and/or *N*-pivaloyl-*o*-benzylaniline. *J. Org. Chem*. 1989, **54**, 509−510.

S2. J. N. Demas, G. A. Crosby The Measurement of Photoluminescence Quantum Yields. *J. Phys. Chem.* 1971, **75**, 991–1024.